Review of 2026-4358, Poncet et al, 'Validation of ATLID stratospheric aerosol retrievals using SAGE III/ISS and ground-based lidar observations'

General: Article is a systematic examination of the stratospheric aerosol retrievals from the EarthCARE ATLID against concurrent accurate reference standards for this difficult to observe region of the atmosphere. It is well written and figures were thoughtfully created. It is a very relevant topic with important conclusions regarding the current ATLID L1 and L2 products for the stratosphere. With clarification of a thread and a few minor corrections it should be accepted for publication.

We thank the referee for the careful reading of our manuscript and for the positive assessment of our work. We are grateful for the constructive comments, in particular on the day/night analysis, which helped us to clarify this part of the paper. Following the referee's suggestions, we have revised the day/night thread (Sect. 3.2.1 and Conclusions) and addressed the minor comments. Our point-by-point responses are given below.

Specific – Major:

1. Day/night performance: The thread related to comparison results when grouped by the solar time of the EarthCARE overpass is interesting, changes the tone as the paper evolves and has some unsupported intermediate conclusions.

We agree that the day/night thread was not treated consistently throughout the paper and that some intermediate conclusions were not supported by the evidence presented. We have revised this part of the manuscript: the unsupported statements have been removed, and Sect. 3.2.1 and the Conclusions have been rewritten so that they are consistent with each other. The details are given in our responses to comments 2 to 7 below.

2. Figure 2 caption says "…(a) daytime and (b) nighttime SAGE III/ISS occultations", but lines 189-191 state day/night definition is for EarthCARE overpass. This is confusing and seems to be two different situations or did I miss something in the discussion of the collocation method that ensured a certain type of occultation is paired with a certain type of ATLID observation. Furthermore, daytime/nighttime occultation is not a common definition and typically the label rise or set (from the viewpoint of the observer) is used. This shouldn't matter for the occultations since the geometry is the same for both types of events. A sunset is sunrise in reverse and the solar zenith angle at each tangent point is 90 degrees, by definition.

The collocation method does not pair a given type of occultation with a given type of ATLID observation. The day/night split refers only to the illumination conditions of the ATLID overpass, and the caption of Fig. 2, which referred to "daytime and nighttime SAGE III/ISS occultations", was incorrect. We agree that this terminology is not appropriate: SAGE III/ISS events are sunrise or sunset occultations with the same geometry, and the expression "daytime/nighttime occultations" is no longer used in the manuscript.

3. Line 203-204: What is the reference for this "well-known increase…during daytime occultations?"

There is no such reference: the statement was incorrect and has been removed. The solar background argument applies to lidar measurements, not to SAGE III/ISS, whose aerosol profiles are obtained from solar occultations at sunrise and sunset under the same measurement geometry.

4. Line 206: "confirming the improved SNR performance of nighttime occultations" Did you mean "nighttime" ATLID observations? Again, I don't know what nighttime solar occultations are and there has been no demonstration of this for SAGE III/ISS. SAGE II did exhibit differences between rise and set retrievals, but that was caused by the thermal sensitivity of that instrument and the

rapidly changing thermal environment coming out of night into day for the rise events. It had nothing to do with the "solar background radiation on the detector."

The day/night classification refers to the ATLID observations: it is based on the solar elevation angle of the collocated EarthCARE overpass (Sect. 3.2.1), not on the SAGE III/ISS occultations, and the expression "nighttime occultations" was therefore incorrect. In addition, the original sentence attributed the larger daytime dispersion to solar background radiation on the SAGE III/ISS detector, which was not supported by our analysis and has been removed. The comparison only shows that the relative differences associated with daytime ATLID overpasses have a larger standard deviation (about 32 %) than those associated with nighttime overpasses (about 17 %); it does not isolate the origin of this difference (see also our responses to comments 6 and 7).

5. Line 207, "well within the altitude-to-altitude variability of the median profiles": What median profiles? Are these the median extinction profiles or median difference extinction profile?

These are the altitude-resolved median profiles of the relative extinction difference, $(\alpha_{L1} - \alpha_{SAGE})/\alpha_{SAGE}$, shown as black lines in Fig. 2, not median extinction profiles. The sentence has been clarified accordingly.

6. Line 209-211: The conclusion drawn is not supported by the evidence cited. It could still be true, but no evidence has been presented to rule-out ATLID having increased noise for 'daylight' observations. Since the day/night definition used in lines 189-191 do not guarantee that there is only one type of occultation in each category. To do that, an additional filter would have to be used. Or the overpasses could be divided in another way and use the occultation definition to divide using sunrise vs. sunset.
    a. To that end a colleague from the SAGE validation team analyzed aerosol profiles from OHP vs. SAGE III/ISS and found no appreciable difference in performance between sunrise and sunset events, with summary plots very similar to that posted on the mission Comparisons webpage that ignores the occultation type: https://sage.nasa.gov/sageiii-iss/browse_images/quicklook/SAGEWeb/Validation/AerosolLidar/Haute_Provence.png.

We agree that the conclusion drawn at lines 209–211 was not supported by the evidence presented, and it has been removed. As the referee points out, the SAGE III/ISS occultation geometry (sunrise vs. sunset) is independent of the daytime/nighttime illumination conditions experienced by the EarthCARE satellite along its orbit, and our day/night split does not separate sunrise and sunset events. We are grateful for the analyses carried out by the SAGE validation team, which show no appreciable difference between sunrise and sunset retrievals. They rule out the explanation given in the original manuscript, and we now cite the referee's comment on this point. We no longer draw any conclusion on the origin of the larger dispersion of the collocations with daytime ATLID overpasses (about 32 % vs. 17 % for nighttime overpasses). We apologize for the incorrect interpretation given in the original manuscript.

    b. For the stratosphere, the SAGE III/ISS solar occultation data can also be compared sunrise vs. sunset for those few times each year (~5) when the occultation latitude overlaps between the two types. Within ~24hrs the same latitude band is sampled by each event. Zonal statistics for the SAGE III/ISS 384 nm aerosol (and other products) for the dates of this article show no appreciable difference between sunrise and sunset retrievals. A similar exercise (comparing daily zonal statistics) using ATLID data should be possible given it runs day and night.

The absence of any appreciable difference between sunrise and sunset retrievals in the SAGE III/ISS zonal statistics for the period of our study confirms that the type of occultation event cannot explain the day/night contrast discussed in Sect. 3.2.1 (see our response to comment 6). We agree that comparing

daily zonal statistics of daytime and nighttime ATLID observations would be an appropriate way to quantify a possible illumination dependence of the ATLID L1 retrieval. This analysis is beyond the scope of the present validation study, but we now mention it as a perspective in the revised manuscript.

7. Lines 402-407: The tone of this is different than when discussed in section 3.2. It stands to reason that the HSRL daytime performance is better than elastic lidar, but not immune from daylight noise. Whereas the occultation performance should be independent of sunrise vs. sunset since they are essentially the same measurement conditions, just reversed in time.

We agree. The Conclusions have been harmonised with the revised Sect. 3.2.1: the difference in dispersion between the collocations with daytime and nighttime ATLID overpasses is now reported without attributing it to either instrument, consistently with our response to comment 6. We also agree with the referee that the HSRL design improves the daytime performance of ATLID compared with elastic lidars without making it immune to daylight noise, and we now state this explicitly. As the referee notes, the SAGE III/ISS performance should not depend on the type of occultation event, since sunrise and sunset measurements are made under the same conditions.

8. Completely agree with lines 375-377 that the comparison results include "the combined uncertainties of both instruments."

No change was needed here.

Specific – Minor:

1. Line 26: Consider adding fundamental HSRL ref.:
   Fiocco and DeWolf https://doi.org/10.1175/1520-0469(1968)025<0488:FSOLEF>2.0.CO;2
   and S. Shipley, D. Tracy, E. Eloranta, J. Trauger, J. Sroga, F. Roesler, and J. Weinman, "High spectral resolution lidar to measure optical scattering properties of atmospheric aerosols. 1: Theory and instrumentation," Appl. Opt. 22, 3716-3724 (1983).

Done. Both references have been added.

2. Line 62: 'baseline BA and its successors BB and BC' What are these items?

BA, BB and BC refer to the EarthCARE processing baselines, i.e. successive versions of the ESA ground-processing chain used to generate the ATLID products. EarthCARE processing baselines are identified by two capital letters: the first letter denotes a major processing/reprocessing generation, while changes in the second letter indicate subsequent incremental updates. Baseline BA corresponds to the first homogeneous reprocessing of the EarthCARE data record using the B-generation processors, while BB and BC contain subsequent updates. We have clarified this terminology in the revised manuscript. Baars et al. (2026) gives a particularly clear definition and was cited here.

3. Line 242: Which sAOD from SAGE was used? The stratospheric_aerosol_optical_depth parameter in the L2 product is occasionally invalid/missing because of an error in the way it is computed from the original aerosol extinction coefficient profile. Hopefully this will be fixed in the future. If you computed SAGE III/ISS sAOD directly from the aerosol profiles, then no worries. Otherwise, you might want to revisit that section of the analysis.

We computed the SAGE III/ISS sAOD directly by integrating the aerosol extinction profiles over the same altitude range as for ATLID (from the ATLID tropopause + 1 km to 30 km); the stratospheric_aerosol_optical_depth parameter of the Level-2 product was not used. This is now stated explicitly in the manuscript.

4. Line 373: Why use 384-521 nm for the Angstrom exponent instead of 384-449 nm? It might produce more stable results.

We tested the sensitivity of our results to this choice over the ATLID observation period. The mean Ångström exponent derived from the 384/521 nm pair is 0.866, compared with 0.704 for the 384/449 nm pair. Using the Ångström law to extrapolate the SAGE III extinction from 384 to 355 nm gives conversion factors of 1.070 and 1.057, respectively. Thus, changing from the 384/521 nm to the 384/449 nm Ångström exponent changes the converted 355 nm extinction by only about 1.3%. This difference is small compared with the variability and uncertainties involved in the ATLID–SAGE III/ISS comparison and does not affect the conclusions of the study. We have added this sensitivity estimate to the revised manuscript.

5. Figure 1b: What does the relative diff. plot look like when plotted as function of tropopause relative altitude? It is not clear where the tropopause is in this figure.

We have updated both Figure 1b (here **Figure R1**) and Figure 2a 2b (here **Figure R2**) to show the relative extinction difference between ATLID L1 and SAGE III/ISS as a function of altitude relative to the local tropopause. To focus on the region immediately above the tropopause, only levels at least 1 km above the local tropopause are retained in the analysis, consistent with the lower limit used for the sAOD integration. The overall median relative differences are consistent with the original absolute-altitude representations (-2.2% for all profiles, -4.2% for daytime, and -0.5% for nighttime). The manuscript text and figure captions have been updated to reflect this new vertical coordinate.

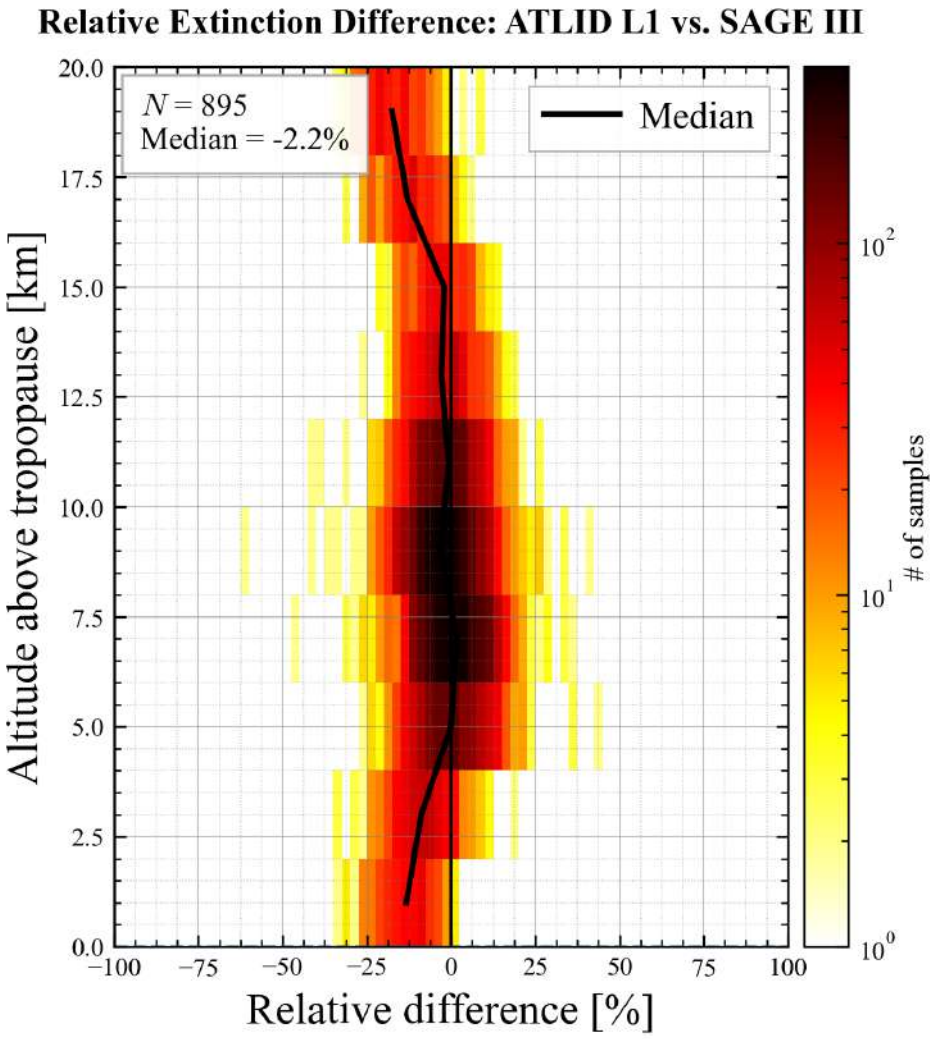



**Figure R1.** Relative extinction difference $(\alpha_{\mathrm{L1}} - \alpha_{\mathrm{SAGE}})/\alpha_{\mathrm{SAGE}}$ between ATLID L1 and SAGE III/ISS as a function of altitude relative to the local tropopause, $z - z_{\mathrm{trop}}$, for the 895 collocated profiles. Levels at least 1 km above the local tropopause are included. The tropopause corresponds to $z - z_{\mathrm{trop}} = 0$ km by definition. The colour scale indicates the number of samples per bin, and the solid black curve shows the median relative difference in each altitude-relative bin.

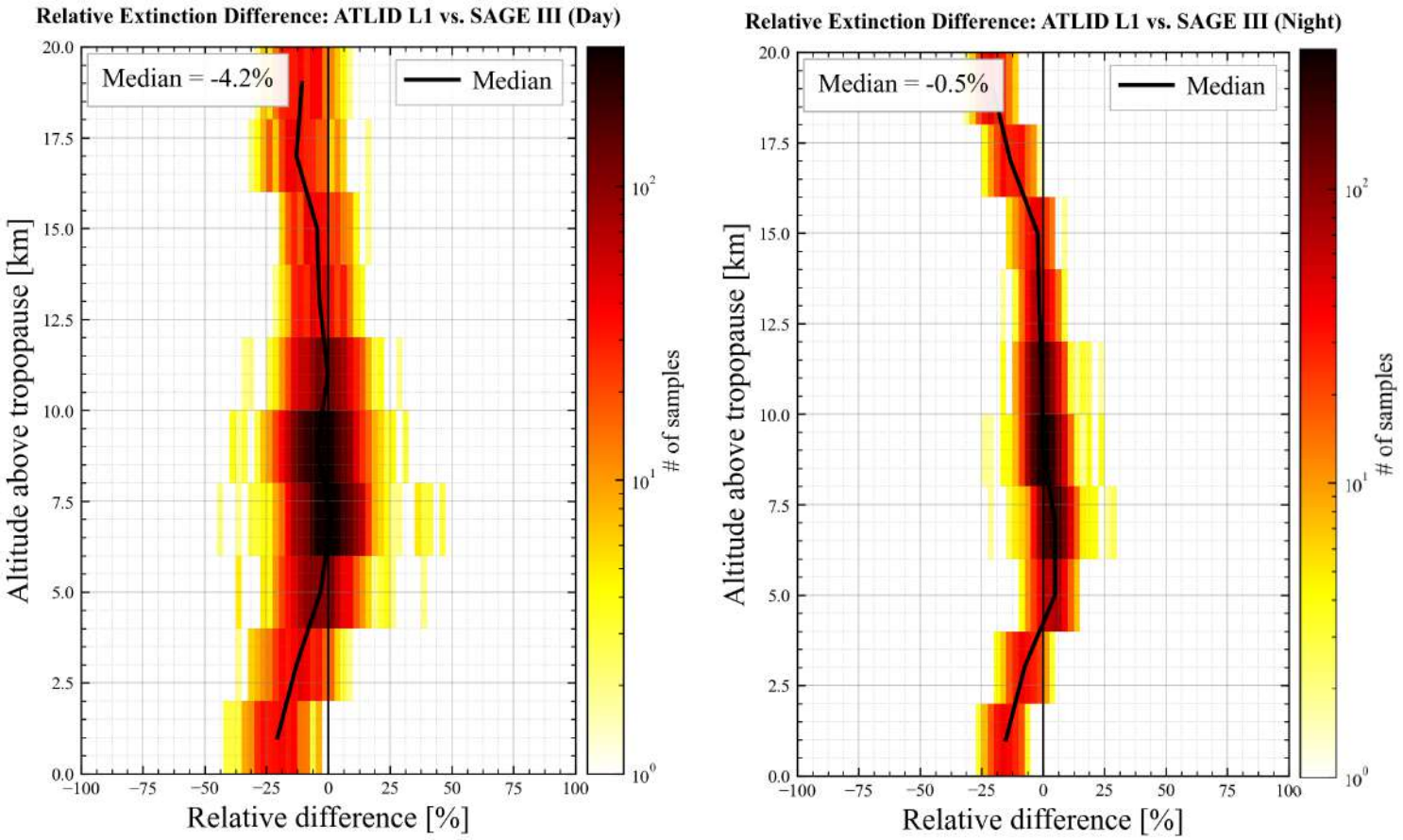



**Figure R2.** Relative extinction difference $(\alpha_{L1} - \alpha_{SAGE})/\alpha_{SAGE}$ between ATLID L1 and SAGE III/ISS as a function of altitude above the local tropopause, shown separately for (a) daytime ATLID overpasses (SEA > 0°) and (b) nighttime ATLID overpasses (SEA ≤ 0°). The colour scale gives the number of samples per bin on a logarithmic scale. The solid black line shows the altitude-resolved median; the inset in each panel reports the overall median relative difference over the displayed altitude range (-4.2% for daytime and -0.5% for nighttime).

Review: Validation of ATLID stratospheric aerosol retrievals using SAGE III/ISS and ground-based lidar observations

The purpose of this paper is to validate the stratospheric aerosol observations from ATLID on EarthCARE through comparison with observations from SAGE III/ISS and two ground-based lidars. Overall, the paper is well written and an important contribution for any users of the ATLID data. I recommend publication after minor revisions.

We sincerely thank the referee for the positive assessment of our manuscript and for the very constructive suggestions, which helped us to improve the paper. We have addressed all comments and detailed our revisions below.

I have two main suggestions:

1. Choice of lidar ratio: the lidar ratio directly scales the backscatter coefficient when calculating the extinction, so using an accurate value is important. The manuscript mentions that a full analysis of the lidar ratio choice is a topic of future work. However, the method this paper proposes to anyone who wishes to use stratospheric ATLID data is highly dependent on the lidar ratio, so I think the impact of the lidar ratio on the biases with SAGE should be explored further here. At the very least, it would be helpful to see the impact of varying the lidar ratio within a reasonable range on the bias between the ATLID and SAGE extinctions for some example profiles, like those in Figure 3. This would also help with verifying the statement on lines 352-354, which suggests that the larger bias in the NH is due to smoke particles that have a lidar ratio other than 50 sr

We agree that the effect of the lidar ratio deserves a more quantitative treatment. First, we would like to clarify that our methodology does not simply assume a constant 50 sr lidar ratio across all profiles. As detailed in Section 2.2, we utilize the ATLID L2-derived lidar ratio wherever it is available and falls within physically realistic bounds (30-90 sr), relying on the 50 sr fallback assumption only when the L2 retrieval fails or returns unphysical values.

Following the referee's suggestion, we have updated Figure 3 to make this approach perfectly transparent and to illustrate the impact of the lidar ratio. We have added a secondary axis (green curve) that displays the actual L2-derived lidar ratio used in our calculations. Furthermore, we added a sensitivity envelope (40-60 sr for background/volcanic profiles, and 40-70 sr for boreal smoke cases) strictly limited to the altitudes where the L2 processor does not provide a valid lidar ratio, meaning the 50 sr fallback was applied.

Regarding the statement on lines 352-354, the revised Fig. 3 gives a more nuanced picture. In the smoke case of Fig. 3c, the L2 provides a lidar ratio of about 60 sr within the smoke layer, and this value is used in the L1-derived extinction; the L1 sAOD (0.036) is then higher than the SAGE III/ISS sAOD (0.024). In the smoke case of Fig. 3d, the L2 provides no valid lidar ratio within the smoke layer (13-20 km), where the 50 sr fallback is used; the L1 sAOD (0.012, or 0.009-0.016 for 40-70 sr) is close to the SAGE III/ISS value (0.013). These examples show that the lidar ratio of smoke

particles alone cannot explain the larger negative bias found in the Northern Hemisphere. Section 4.1 has been revised accordingly: the lidar ratio of smoke is mentioned as one possible contribution, and a dedicated analysis comparing the summer 2025 smoke period with the rest of the record is left for future work.

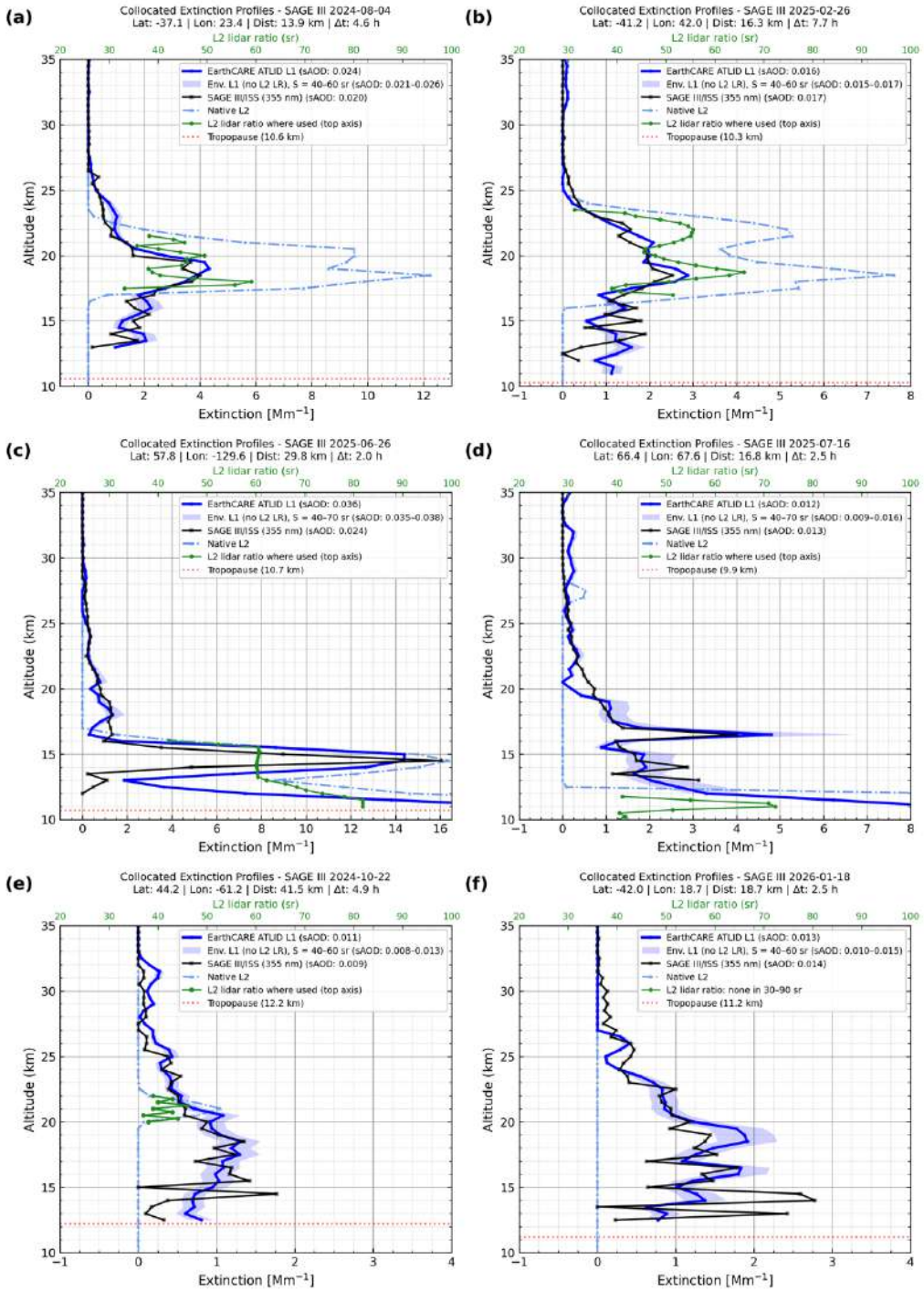


**Figure 3.** Collocated extinction profiles from SAGE III/ISS, ATLID L1, and native ATLID L2 for selected case studies: (a, b) Southern Hemisphere Ruang volcanic plume, (c, d) boreal wildfire smoke, and (e, f) background aerosol conditions. The green curve (top axis) shows the actual L2-derived lidar ratio applied in the L1 calculation where valid (30-90 sr). The shaded blue envelopes represent the L1 extinction sensitivity to the assumed lidar ratio, using a range of 40-60 sr for the volcanic and background cases (panels a, b, e, f) and 40-70 sr for the smoke cases (panels c, d), and are shown exclusively at altitudes where a valid L2 lidar ratio is unavailable. The horizontal dotted pink line indicates the local tropopause altitude. Dist is the great-circle distance between the SAGE III/ISS tangent point and the closest of the averaged ATLID profiles (all within 50 km), and Δt is the time difference between the SAGE III/ISS event and each collocated ATLID overpass.

2. Organization of results (Section 3): As a user of the ATLID data, my initial thought would be to use the L2 product, and I believe this paper is the first to clearly demonstrate the problems with the L2 aerosol retrieval in the stratosphere. Therefore, I think it would be helpful to show the L1/L2 comparison at the start of the paper, which would then motivate the detailed validation of the L1-derived extinction. This could be done by moving Figures 3 and 7 and the surrounding discussion to the start of Section 3, so that the issues with the L2 product are immediately clear.

We considered this suggestion carefully, but we prefer to keep the current order of Section 3. The L2 sAOD comparison (Fig. 7) uses the same matchups as the L1 comparison (Fig. 4) and is discussed relative to it, so it is easier to follow once the L1 results have been presented. In addition, the limitations of the L2 product are already stated in Sect. 2.2 (lines 65-68, rewritten following Referee #3), where they motivate the L1-based retrieval. To make them clear from the start of the results, we have added a short paragraph at the beginning of Section 3 that summarizes them, with pointers to Sects. 3.2.2 and 3.6.

Specific comments:

- Line 62: An explanation of the baselines and the difference between them would be helpful.

BA, BB and BC refer to the EarthCARE processing baselines, i.e. successive versions of the ESA ground-processing chain used to generate the ATLID products. EarthCARE processing baselines are identified by two capital letters: the first letter denotes a major processing/reprocessing generation, while changes in the second letter indicate subsequent incremental updates. Baseline BA corresponds to the first homogeneous reprocessing of the EarthCARE data record using the B-generation processors, while BB and BC contain subsequent updates. We have clarified this terminology in the revised manuscript. Baars et al. (2026) gives a particularly clear definition and was cited here.

- Section 2.2: I think it is worth providing more details on the method used to calculate the extinction coefficient, even if it is a repeat of Khaykin et al (2026), given that one of the main recommendations in this paper is to derive extinctions from the L1 observations instead of using the official ATLID product.

We agree. Given that the L1-based derivation is the core recommendation of this paper, we have expanded Section 2.2 to provide a more detailed, step-by-step description of the unattenuated particulate backscatter retrieval from the molecular reference profile, rather than relying solely on the citation.

- Comparison with ground-based observations: What is the impact of using a fixed lidar ratio of 50 sr to convert these observations to extinction/SAOD, when the ATLID observations are (at least sometimes) converted to extinction using the retrieved L2 lidar ratio?

For the sAOD comparison against ground-based lidars, the ATLID L2 lidar ratio is used only where it lies within 30-90 sr; elsewhere, ATLID uses the same 50 sr value as the conversion of the ground-based profiles, so the two conversions differ only at these levels (see also our response to Referee #3, comment 2). More importantly, to rigorously isolate the performance of the ATLID retrieval from any lidar-ratio assumptions, our profile-level comparison against OHP and TMF (Section 3.5) is performed directly on the backscatter coefficients. This independent backscatter comparison reproduces the same bias structure, confirming that the bias originates in the Level-1 scattering-ratio retrieval itself rather than in the lidar ratio conversion. We have clarified this distinction in the text.

- Are data points below the tropopause removed before calculating the relative difference in extinction? (Figures 1 and 2)

Yes. Following suggestions from Referees #1 and #3, we have updated Figs. 1b and 2 to display the relative difference as a function of altitude *relative to the local tropopause*, strictly retaining only levels at least 1 km above the local tropopause (consistent with the sAOD integration limits).

- Figure 2 caption: the meaning of daytime and nighttime SAGE III occultations is not clear, given that the measurements are at sunrise and sunset. Also, the text on line 189 says that the split is based on the EarthCARE overpass time, not the SAGE III occultation time. Please clarify this.

The referee is correct. The day/night split refers exclusively to the illumination conditions of the ATLID overpass (based on the solar elevation angle), not the SAGE III/ISS occultations. SAGE III/ISS events are sunrise or sunset occultations with the same geometry. The caption of Fig. 2, which incorrectly referred to "SAGE III/ISS occultations", has been corrected to "daytime and nighttime ATLID overpasses", and the text in Section 3.2.1 has been revised to remove this ambiguity.

- Line 194: Was it unexpected for the day and night bias to have a similar vertical structure? If so, this should be explained, and if not, I would remove the word “remarkably”.

It was not unexpected: the vertical structure of the bias is mainly governed by factors common to both subsets, such as the vertical distribution of the aerosol loading and the altitude relative

to the tropopause. The word "remarkably" has been removed, and the paragraph has been rewritten for the new tropopause-relative version of Fig. 2 (see our response to Referee #1, minor comment 5).

- Figure 3 caption: this figure is very insightful, but discussions of the bias between L1/L2 and SAGE should be in the main text, not the figure caption.

Done. We have streamlined the caption and moved the detailed profile-by-profile analysis into the main text (Sect. 3.2.2).

- Section 3.3: Do you have any theories as to why ATLID overestimates the SAOD in cases with more aerosol?

We thank the referee for this question. We see two possible contributions, which are now discussed in Sect. 3.3.
(i) Coverage of the lowermost stratosphere. Both sAODs are integrated from the tropopause + 1 km to 30 km, but in dense layers the lowest SAGE III/ISS levels are more likely to be removed by the quality screening (e.g. aerosol–cloud mixture flag) or not retrieved at all, as the transmission along the line of sight decreases. The ATLID L1 profile retains these levels. When a dense layer lies just above the tropopause, as in Fig. 3c, where ATLID shows large extinction values between the tropopause and 12.5 km that are absent from the SAGE III/ISS profile, the ATLID sAOD therefore includes a contribution that is missing from the SAGE III/ISS sAOD.
(ii) Sampling geometry. SAGE III/ISS integrates along a limb path of a few hundred kilometres, whereas the ATLID extinction is an average of nadir profiles within 50 km. For compact plumes, ATLID can sample the core of the plume while SAGE III/ISS sees it diluted along its line of sight, which produces large positive differences; in the opposite case, the negative difference is limited by this dilution. This favours a positive tail at high aerosol loading.

- Figures 4 and 7: displaying the comparison with SAGE III in a histogram form, as was done for Figure 1a, would be helpful for understanding these figures. Currently, it is difficult to determine the range of SAOD values where the agreement is best.

We followed this suggestion. In the revised Figs. 4 and 7, the SAGE III/ISS matchups are shown as 2D histograms (number of matchups per 0.001 × 0.001 bin, logarithmic colour scale), as in Fig. 1a. The few TMF and OHP matchups are still shown as individual symbols. To show directly where the agreement is best, we also added the median ATLID sAOD in 0.002-wide classes of SAGE III/ISS sAOD (classes with at least five matchups), with the interquartile range as error bars.

Above about 0.02, few matchups remain and the interquartile range widens. For L2, about half of the matchups (321 of 652) have sAOD_L2 = 0, so the class medians in Fig. 7a stay close to zero over most of the sAOD range. When these cases are excluded (Fig. 7b, N = 331), the class medians fall on both sides of the 1:1 line with wide interquartile ranges, and no sAOD range of consistent agreement emerges. This is now stated in Sects. 3.3 and 3.6.

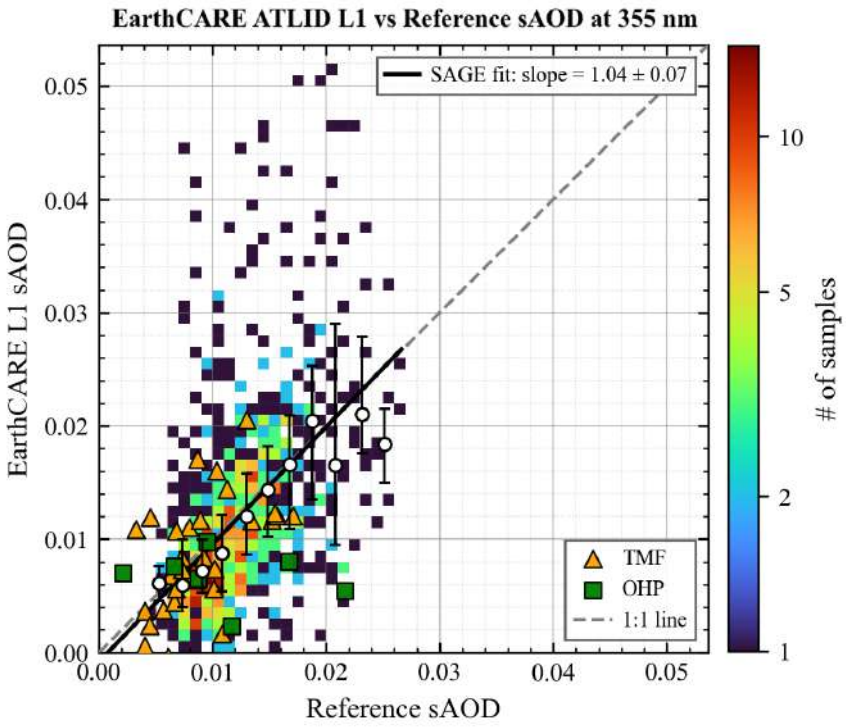



**Figure 4.** ATLID L1 sAOD versus reference sAOD, integrated from the ATLID-derived tropopause +1 km to 30 km. SAGE III/ISS matchups (N = 895) are shown as a 2D histogram (number of matchups per 0.001 × 0.001 bin, logarithmic colour scale); TMF (triangles) and OHP (squares) matchups are shown individually. White circles give the median ATLID sAOD in 0.002-wide classes of SAGE III/ISS sAOD (classes with at least five matchups), with the interquartile range as error bars. The dashed grey line is the 1:1 reference. The solid black line shows the linear regression fit to the SAGE III/ISS matchups: slope = 1.04 ± 0.07 (±1 standard error), intercept = (−0.8 ± 0.9) × $10^{-3}$, R = 0.67.

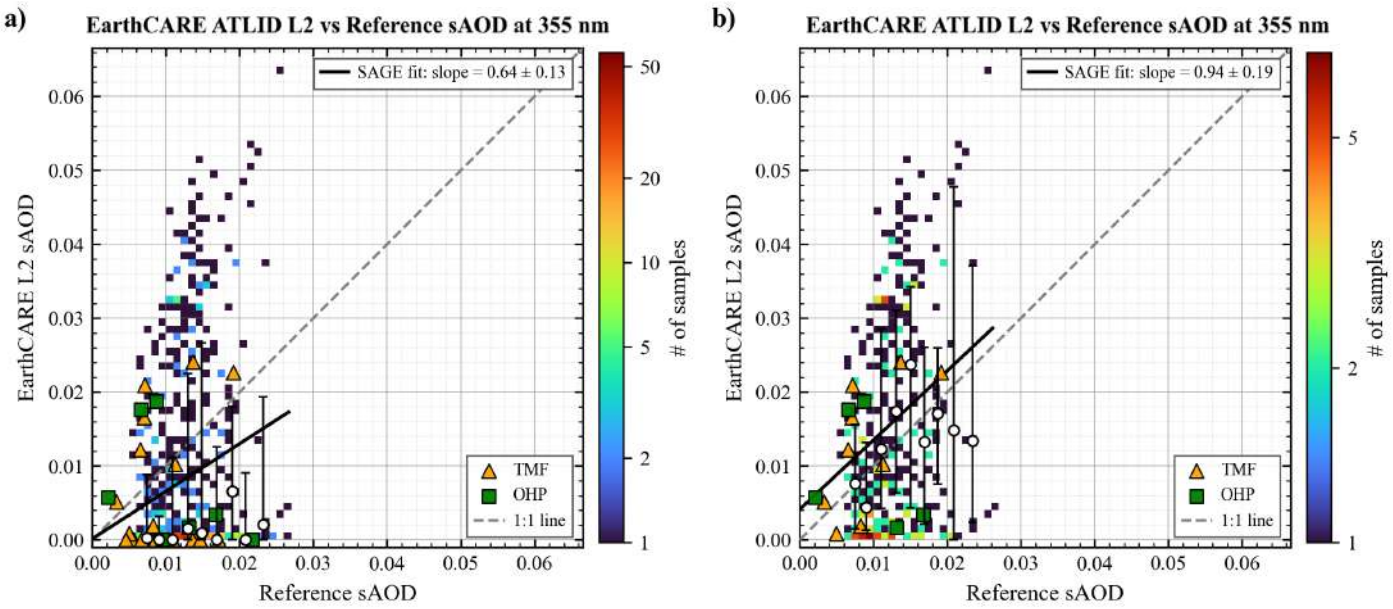



**Figure 7.** Native ATLID L2 sAOD versus reference sAOD, integrated from the ATLID-derived tropopause +1 km to 30 km. SAGE III/ISS matchups are shown as a 2D histogram (number of matchups per 0.001 × 0.001 sAOD bin, logarithmic colour scale), and TMF (triangles) and OHP (squares) matchups are shown individually. White circles give the median ATLID L2 sAOD in 0.002-wide classes of SAGE III/ISS sAOD (classes with at least five matchups), with the interquartile range as error bars. **(a)** All collocated matchups, including cases for which the L2 processor returns no stratospheric retrieval (sAOD_L2 = 0, in the bottom row of the histogram, along the horizontal axis). The linear regression fit to the SAGE III/ISS matchups (N = 652; solid black line) yields a slope of 0.64 ± 0.13 and an intercept of (0.1 ± 1.7) × $10^{-3}$ (R = 0.19). **(b)** Same comparison but restricted to actual retrievals (sAOD_L2 > 0); the null retrievals (sAOD_L2 = 0) shown along the horizontal axis in panel (a) are here excluded from the display, the class medians and the fit. The regression to the SAGE III/ISS matchups (N = 331) then yields a slope of 0.94 ± 0.19 with a positive intercept of (4.1 ± 2.6) × $10^{-3}$ (R = 0.26). In both panels, the dashed grey line is the 1:1 reference, the slope of the fit is given in the upper-right corner, and quoted uncertainties are one standard error. The L2 comparison includes fewer SAGE III/ISS matchups than the L1 comparison of Fig. 4 because the daily L2 files contain fewer profiles than the L1 files (about 6,400 vs. 22,750 per day).

- Line 267: it looks like the gray shaded region is the broadest in the NH tropics/midlatitude (10N-30N) and narrowest at higher latitudes. Is this sentence phrased backwards?

The referee is right, the sentence was phrased backwards. The ±2 SE envelope is narrowest where the collocations are dense (mid-latitudes) and broader where sampling is sparse. The text has been corrected to accurately reflect the figure.

Specific comments:

- Line 148: Change “the following metrics” to “the metrics in Table 1.”
- Line 154: remove comma after “independent”
- Section 3.2.2: Include “=” sign between “lat” and the value in all cases.

Done. We have implemented all three technical corrections in the revised manuscript.

This paper presents a validation of the EarthCARE ATLID stratospheric aerosol extinction profiles and stratospheric aerosol optical depth by comparison against SAGE III/ISS solar occultation measurements and the ground based lidars at the Table Mountain Facility and the Observatoire de Haute-Provence. The paper is well organized and presents an important validation of the ATLID stratospheric aerosol retrievals. After edits for clarification and readability I recommend this paper for publication.

We thank the referee for the careful reading of our manuscript and for the positive assessment of our work. The comments helped us to improve the clarity of the paper; in particular, following the referee's suggestion, the profile comparisons with SAGE III/ISS are now presented as a function of altitude relative to the local tropopause. Our point-by-point responses are given below.

General comments

1. **Analysis in altitude above tropopause** – When analyzing vertical profiles from scattered latitudes it is sometimes clearer to present analysis in altitude above tropopause. This may make the features in your altitude plots more distinct and give the reader more confidence in your statements with respect to altitude. Such as the statements made in section 3.2, which discuss features at specific altitudes. With geometric altitude the altitude plots may be spreading out the near tropopause features. As well the latitude plot (Figure 5a) may be affected by this.

Following the referee's suggestion (also made by Referee #1, minor comment 5), Figs. 1b and 2 now show the relative extinction difference as a function of altitude relative to the local tropopause, using the ATLID tropopause height and all levels located at least 1 km above it. As anticipated by the referee, this representation changes the picture near the tropopause. The moderately positive bias found at 10–13 km in geometric altitude, which relied on a small number of profiles with a low tropopause, is no longer present. The median relative difference is negative in the first ~3 km above the tropopause (about −10 to −15 %), close to zero between about 5 and 15 km above the tropopause, and negative again further up. The overall median relative difference is essentially unchanged (−2.2 %, compared with −2.3 % in geometric altitude), since only the vertical coordinate differs. The description of the vertical structure in Sect. 3.2, its discussion in Sect. 4.1, the abstract and the conclusions have been revised accordingly. In particular, near the tropopause the SAGE III/ISS comparison now agrees with the ground-based lidars, which also show a negative bias just above the tropopause, so the SAGE-specific explanations proposed in Sect. 4.1 for a positive offset are no longer needed.
Regarding Fig. 5a, the sAOD of each matchup is integrated from 1 km above the local tropopause to 30 km, so the lower bound of the integration already follows the tropopause.

The latitudinal distribution of the sAOD bias is therefore not affected by the geometric-altitude representation in the same way as the profiles, and Fig. 5a has been kept in its present form.

2. **Use of the L2 lidar ratio in the L1-derived extinction**– Problems with L2 extinction are well discussed, however the L2 lidar ratio is used in calculating the L1-derived extinction. Could the issues affecting the L2 retrieval be of any concern for the L1-derived values through the use of the L2 lidar ratio? What are the possible effects on the resulting error? A short discussion of this seems warranted.

We agree that this point deserved a discussion, which has been added to Sect. 2.2. The L2 lidar ratio enters the L1-derived extinction only at the levels where it is available and lies between 30 and 90 sr; elsewhere, a value of 50 sr is used. The issues affecting the L2 retrieval can therefore affect the L1-derived product only at these levels, and only through the lidar ratio, not through the L2 extinction itself. Since the extinction is proportional to the lidar ratio, a relative error on the lidar ratio gives the same relative error on the extinction; with the 30-90 sr bounds, an erroneous L2 value can change the extinction by −40 % to +80 % relative to the 50 sr value at the levels concerned. Finally, the backscatter comparison with the ground-based lidars (Sect. 3.5) does not involve any lidar ratio and shows the same negative bias just above the tropopause, which indicates that the main features of the comparison are not driven by the L2 lidar ratio. See also our response to the first main comment of Referee #2, where the effect of the lidar ratio is illustrated for the case studies of Fig. 3.

Specific Comments

3. **Section 3.2: noise-floor interpretation** – The statements that the scatter at low extinction is "consistent with the additive retrieval noise floor" and that the relative differences approach zero above 25 km as both instruments approach their respective noise floors could use more explanation or supporting references. In particular, it is not obvious why approaching the noise floor should cause the relative difference between the instruments to approach zero. Some additional justification of this interpretation would be helpful.

We agree that these two statements needed clarification.

(i) By "additive noise floor" we meant the random noise of the ATLID L1 extinction, which comes from the detection noise of the ATLID channels (in particular the Mie channels, whose signal is weak in the stratosphere) and whose absolute magnitude does not depend on the aerosol loading. A random error of roughly constant absolute magnitude produces a constant absolute scatter, and therefore a relative scatter that increases as the extinction

decreases. This is why the scatter in Fig. 1a is largest, in relative terms, at low SAGE III/ISS extinction. The sentence has been rewritten to explain this.

(ii) We agree with the referee that approaching the noise floor should increase the scatter of the relative differences, not bring their median toward zero, and this interpretation has been removed. Moreover, with the tropopause-relative coordinate now used in Fig. 1b (see our response to general comment 1), the median relative difference no longer converges toward zero at the highest levels: it is close to zero between about 5 and 15 km above the tropopause and becomes negative further up. The revised Sect. 3.2 describes this behaviour without invoking the noise floor, and the corresponding sentence in Sect. 4.1 has been removed.

4. **Figure 7 / treatment of missing L2 retrievals** – The text describes unsuccessful L2 retrievals as fill values, while Figure 7 appears to assign zero sAOD to cases where no stratospheric retrieval is returned. It would be helpful to clarify exactly how these cases are handled. Are fill values explicitly converted to zero during the sAOD calculation, or does the L2 product actually report zero extinction? It would also be useful to explain why Figure 7 contains 652 SAGE comparisons when the overall collocation dataset contains 895 profiles.

The L2 product itself reports zero extinction at the levels where no aerosol is detected, and these zeros are used as such in the sAOD integration: sAOD_L2 = 0 therefore means that the L2 extinction is zero at all levels of the integration range. True fill values are rare (about 2–5 % of the stratospheric levels) and are discarded, not converted to zero. The manuscript wrongly referred to these cases as fill values; this has been corrected.

The L2 comparison includes fewer matchups (652) because the daily L2 files used here contain fewer profiles than the L1 files: about 6,400 profiles per day for L2, compared with about 22,750 for L1. This is now explained in Sect. 3.6 and in the caption of Fig. 7.

5. **Line 51: “season”.** “time” would be more appropriate I think, there is no real seasonal analysis.

Agreed. "Season" has been replaced by "time" (line 51).

6. **Dist in the Figure 3 extinction plots** – I like this detail added to the plot. Am I right in thinking this is the distance between the SAGE tangent point and ATLID’s footprint? If so, this should be stated somewhere. Since multiple ATLID profiles are averaged for each collocation, it would also be helpful to clarify exactly how this distance is defined.

Yes. "Dist" is the great-circle (haversine) distance between the SAGE III/ISS tangent point and the closest of the ATLID profiles averaged in the collocation; all the averaged ATLID profiles lie within 50 km of the tangent point (Sect. 2.5). This definition is now given in Sect. 2.5 and in the caption of Fig. 3. In addition, the time difference Δt shown in the panel titles is now computed from the time of the collocated ATLID overpass (it was previously computed from the median time of the daily ATLID file, a mistake), and the corrected values are reported in Sect. 3.2.2.

7. **lines 67–68: "Successfully retrieves extinction".** Seems to be too strong a statement, or perhaps just accidentally misleading, considering what is said about the performance later in the paper.

We agree that this wording was misleading. Lines 65–68 have been rewritten as: "However, as suggested by Khaykin et al. (2026) (hereafter K26) and confirmed in this study, the L2 processor frequently returns zero extinction under low-aerosol background conditions, in the absence of a sufficiently strong aerosol signal. For optically thicker layers such as volcanic plumes, the L2 algorithm does return non-zero extinction, but it overestimates the peak extinction (Sect. 3.2.2), and the resulting sAOD is only weakly correlated with the reference measurements (Sect. 3.6)."

8. **Lines 382–384:** The statement that "the true physical lidar ratio is expected to be close to the 50 sr assumed value" should be supported by a reference, or the language softened. Kremser et al. (2016), cited earlier, reports typical stratospheric lidar ratios of approximately 45–50 sr at 532 nm. Since ATLID operates at 355 nm, please clarify whether there is evidence that 50 sr is similarly representative at this wavelength for the aerosol conditions considered here.

We agree that this statement was too strong and have softened it. Direct estimates of the lidar ratio of stratospheric sulfate at 355 nm are scarce. Vaughan et al. (2021) retrieved the 2019 Raikoke and Ulawun sulfate layer at 355 nm with a lidar ratio of 40 sr (50 sr on two nights), checked against Raman measurements on a few nights. A constant value of 50 sr, representative of sulfate aerosol, is also used for the 355 nm LiO3S lidar at Maïdo (Khaykin et al., 2026; K26). The 50 sr value thus lies at the upper end of the values used at 355 nm. Because the L1-derived extinction scales linearly with the lidar ratio, a ±10 sr departure from 50 sr changes the extinction by ±20 %. This sensitivity is now shown as an envelope in the revised Fig. 3, at the levels where the 50 sr fallback is used (40-60 sr for the background and volcanic cases, 40-70 sr for the smoke cases; see also our response to Referee #2, main comment 1).

# Validation of ATLID stratospheric aerosol retrievals using SAGE III/ISS and ground-based lidar observations

Eddy A. Poncet[1,2], Sergey M. Khaykin[1], Sophie Godin-Beekmann[1], and Thierry Leblanc[3]

[1]LATMOS/IPSL, CNRS, UVSQ Université Paris-Saclay, Sorbonne Université, Guyancourt, France
[2]École Centrale de Lyon / Université Claude Bernard Lyon 1, France
[3]Jet Propulsion Laboratory, California Institute of Technology, Wrightwood, CA, USA

**Correspondence:** Sergey M. Khaykin (sergey.khaykin@latmos.ipsl.fr)

**Abstract.** We present a systematic validation of EarthCARE ATLID stratospheric aerosol retrievals against SAGE III/ISS and ground-based lidars at the Table Mountain Facility (TMF) and the Observatoire de Haute-Provence (OHP), using 895 SAGE III/ISS, 55 TMF, and 26 OHP collocations over August 2024-April 2026 and spanning background, volcanic, and wildfire smoke conditions. We evaluate a Level-1-based extinction product, derived directly from the ATLID L1 scattering ratio. Against SAGE III/ISS, this L1 product yields a regression slope of 1.04 for the stratospheric aerosol optical depth (sAOD) and an overall median relative extinction difference of ~~$-2.3\,\%$~~$-2.2\,\%$; across all matchups, the relative sAOD bias has a global mean of $-3.2\,\%$ with a standard deviation of $65.7\,\%$. ~~The altitude-resolved comparison reveals a moderate positive bias near the tropopause ($\sim +10\,\%$), a pronounced negative excursion of up to $-15\,\%$ in the lower-to-mid stratosphere, and convergence toward near-zero bias above~~ As a function of altitude above the local tropopause, the median relative difference is negative in the first ~~25~~3 km ~~, together with~~ above the tropopause (about $-10\,\%$ to $-15\,\%$), close to zero between about 5 and 15 km above the tropopause, and negative again further up; the sAOD comparison also shows a systematic negative ~~sAOD~~ bias in the Northern Hemisphere extratropics that increases with latitude. Independent backscatter comparisons against TMF and OHP ~~reproduce the same negative bias in the lower-to-mid stratosphere~~ (also show a negative bias just above the tropopause (overall median differences of $-5.5\,\%$ and $-10.6\,\%$, respectively), indicating that this feature originates in the Level-1 scattering-ratio retrieval itself rather than in the extinction-conversion step. Daytime collocations are markedly noisier than nighttime ones (relative-difference standard deviation of $\sim$32 % versus $\sim$17 %), although the median bias remains close to zero in both cases. In contrast, the native L2 product achieves a regression slope of only 0.64 against SAGE III/ISS sAOD, largely driven by frequent null retrievals under low-aerosol conditions. Even when excluding these missed detections, the correlation remains weak ($R = 0.26$), and the L2 product systematically overestimates peak extinction in dense plumes, making it unreliable for stratospheric monitoring in its current processing baseline.

## 1 Introduction

The EarthCARE satellite mission, launched on 28 May 2024 as part of a collaboration between ESA (European Space Agency) and JAXA (Japan Aerospace Exploration Agency), carries four co-aligned instruments designed to characterize clouds, aerosols, and radiation from space (Wehr et al., 2023). Among these, the Atmospheric Lidar (ATLID) operates at

355 nm and provides vertically resolved profiles of aerosol backscatter, extinction, and depolarization ratio with an unprecedented combination of sensitivity and global coverage (ESA Earth Online, 2026). ATLID's high-spectral-resolution lidar (HSRL) capability allows the independent retrieval of the backscatter and extinction coefficients without prior assumptions on the lidar ratio, representing a significant advancement over conventional elastic-backscatter lidars ~~(Eisinger et al., 2024)~~ (Fiocco and DeWolf, 1968; Shipley et al., 1983; Eisinger et al., 2024).

Stratospheric aerosols play a well-recognized role in climate variability and ozone chemistry, modulating the Earth's radiative budget and providing surfaces for heterogeneous chemical reactions (Kremser et al., 2016). Long-term monitoring of the stratospheric aerosol layer requires accurate, well-characterized observations from multiple platforms. Ground-based lidar networks such as NDACC (Network for the Detection of Atmospheric Composition Changes) provide continuous vertically resolved measurements at fixed locations (NDACC, 2026), while solar occultation instruments aboard satellites, most notably the Stratospheric Aerosol and Gas Experiment (SAGE) series, have historically provided the backbone of global stratospheric aerosol climatologies (Thomason and Knepp, 2023). The SAGE III instrument aboard the International Space Station (SAGE III/ISS), operational since 2017, continues this legacy by delivering high-quality extinction profiles at multiple wavelengths, from which 355 nm extinction can be derived.

The validation of ATLID stratospheric aerosol retrievals is a critical step before the data can be used for scientific applications. Complementary case-study validations of the operational ATLID Level-2 aerosol profiling products against ground-based lidars have recently been reported in the troposphere (Baars et al., 2026), whereas a systematic assessment in the stratosphere (the focus of the present study) is still lacking. This is particularly challenging in background conditions, where the aerosol signal is weak compared to molecular scattering. To address these challenges and thoroughly assess the official Level-2 (L2) performance, an alternative approach based on Level-1 backscatter signals and Rayleigh backscatter from meteorological data, described in Khaykin et al. (2026), is utilized to allow robust extinction retrieval even under low-aerosol conditions.

The study period (August 2024 - April 2026) encompasses a diverse range of atmospheric conditions in the stratosphere, including background aerosol, the volcanic plume from the eruption of Ruang volcano (Indonesia) in April-May 2024 (Khaykin et al., 2026), and intense wildfire smoke injections into the lower stratosphere during the boreal summer of 2025 (Haarig et al., 2026). This variety offers a unique opportunity to assess ATLID's performance across contrasting aerosol regimes and to identify potential sources of systematic discrepancy between ATLID and independent observations.

In this paper, we present a systematic comparison of ATLID-derived stratospheric aerosol extinction and scattering ratio profiles with collocated SAGE III/ISS observations and ground-based lidar measurements from the Table Mountain Facility (TMF, California) and the Observatoire de Haute-Provence (OHP, France). We characterize the absolute and relative bias between ATLID and the reference instruments as a function of altitude, latitude, ~~season~~time, and aerosol loading, and we discuss the potential origins of observed discrepancies. The paper is organized as follows. Section 2 describes the instruments and data used in this study, the collocation methodology, and the comparison metrics. Section 3 presents the comparison results. Section 4 discusses the sources of the observed bias. Section 5 provides the conclusions.

## 2 Data and Methods

### 2.1 The EarthCARE mission and ATLID instrument

Detailed descriptions of the EarthCARE mission and the ATLID instrument are provided by Wehr et al. (2023) and ESA Earth Online (2026); here we summarise only the characteristics relevant to the present study. EarthCARE orbits at approximately 393 km altitude in a sun-synchronous orbit with a 25-day repeat cycle. ATLID provides vertically resolved profiles of aerosol scattering ratio, backscatter, extinction, and linear depolarisation ratio with a vertical resolution of approximately 100 m below 20 km and 500 m above, and a nominal along-track horizontal resolution of approximately 285 m for single shots. For all ATLID products used in this study, we relied on ~~baseline BAand its successors~~ the EarthCARE processing baselines BA, BB and BC, i.e. successive versions of the ESA ground-processing chain. Baselines are identified by two letters: the first denotes a major processing/reprocessing generation, and changes in the second indicate incremental updates. BA corresponds to the first homogeneous reprocessing of the EarthCARE data record with the B-generation processors, while BB and BC contain subsequent updates (Baars et al., 2026).

### 2.2 ATLID Level-1 extinction retrieval

The official ATLID Level-2 (L2) product provides aerosol extinction profiles derived from the HSRL (Donovan et al., 2024). However, as suggested by Khaykin et al. (2026) (hereafter K26) and confirmed in this study, the L2 processor frequently ~~fails to produce valid stratospheric retrievals~~ returns zero extinction under low-aerosol background conditions, ~~defaulting to fill values~~ in the absence of a sufficiently strong aerosol signal. ~~In contrast, the L2 algorithm successfully retrieves extinction for~~ For optically thicker layers such as volcanic plumes, the L2 algorithm does return non-zero extinction, but it overestimates the peak extinction (Sect. 3.2.2), and the resulting sAOD is only weakly correlated with the reference measurements (Sect. 3.6). To overcome this limitation and enable a systematic comparison across all aerosol regimes, we derive ATLID aerosol extinction directly from the Level-1 scattering ratio (SR) using the K26 method. This method retrieves the unattenuated particulate backscatter coefficient ~~$\beta_{\mathrm{aer}}$~~ $\beta_{aer}$ from the molecular reference profile ~~, which is itself computed from ECMWF meteorological~~ in three steps. First, the HSRL design of ATLID separates the particulate (Mie) and molecular (Rayleigh) contributions to the backscattered signal; since both are attenuated by the same two-way transmission, the ratio of the particulate attenuated backscatter (sum of the co-polar and cross-polar Mie signals of the L1 product) to the Rayleigh attenuated backscatter is free of attenuation and equals the ratio $\beta_{aer}/\beta_{mol}$ of the unattenuated particulate and molecular backscatter coefficients. Second, the molecular backscatter coefficient $\beta_{mol}$ is computed for Rayleigh scattering at 355 nm from the ECMWF pressure and temperature profiles provided with the Level-2 data~~and~~ , interpolated onto the ATLID vertical grid. Third, $\beta_{aer}$ is obtained by multiplying the attenuation-free ratio by $\beta_{mol}$, i.e. $\beta_{aer} = (\beta'_{Mie}/\beta'_{Ray})\,\beta_{mol}$. The aerosol extinction coefficient $\alpha_{\mathrm{aer}}$ is then obtained as:

$$\alpha_{\mathrm{aer}}(z) = S_{\mathrm{aer}} \cdot \beta_{\mathrm{aer}}(z), \tag{1}$$

where $S_{\mathrm{aer}}$ is the lidar ratio. Because this derivation relies entirely on non-attenuated inputs derived from the molecular signal, the resulting extinction profiles are free from cumulative attenuation errors inherent to elastic-backscatter lidar inversions, though they remain sensitive to the lidar ratio.

The aerosol extinction coefficient is derived from the ATLID L1 particulate backscatter coefficient using Eq. (1). Wherever the ATLID L2 lidar ratio is available and falls within physically realistic bounds (30-90 sr), it is used directly in the retrieval. In all other cases, including ~~profiles for which~~ levels where the L2 processor returns ~~fill values or unphysical estimates~~zero extinction (no aerosol detected) or unphysical lidar ratios, a constant fallback value of 50 sr is applied, consistent with values reported in the literature for aged stratospheric sulfate aerosols (Kremser et al., 2016) ~~. The sensitivity of the retrieved extinction~~ (see Sect. 4.2 for the 355 nm case). The L2 lidar ratio therefore enters the L1-derived extinction only at the levels where it is available and lies between 30 and 90 sr, so issues affecting the L2 retrieval can affect the L1-derived product only at these levels, and only through the lidar ratio, not through the L2 extinction itself. Since the extinction is proportional to the lidar ratio, ~~and in particular the impact of using a spatially variable~~ a relative error on the lidar ratio gives the same relative error on the extinction; with the 30-90 sr bounds, an erroneous L2 value can change the extinction by $-40\,\%$ to $+80\,\%$ relative to the 50 sr value at the levels concerned. The backscatter comparison with the ground-based lidars (Sect. 3.5) does not involve any lidar ratio and shows the same negative bias just above the tropopause, which indicates that the main features of the comparison are not driven by the L2 lidar ratio~~versus the fixed fallback, is~~ . The sensitivity of the retrieved extinction to the lidar ratio is illustrated for the case studies of Fig. 3 and discussed in Sect. ~~4~~4.2.

Individual ATLID Level-1 profiles within each collocation window (see Sect. 2.5) are averaged to reduce random noise, and a 3-point boxcar smoothing is applied in the vertical dimension to the resulting mean profile. This smoothing improves the signal-to-noise ratio at stratospheric altitudes without significantly degrading the vertical resolution relevant to the features of interest.

### 2.3 SAGE III/ISS

The Stratospheric Aerosol and Gas Experiment III aboard the International Space Station (SAGE III/ISS) has been operational since June 2017 (Cisewski et al., 2014). It measures solar and lunar occultation spectra to retrieve vertically resolved profiles of aerosol extinction, ozone, water vapour, and other trace gases (Thomason and Knepp, 2023). The solar occultation technique provides self-calibrating, high-accuracy measurements with a vertical resolution of approximately 0.5 km. SAGE III/ISS delivers approximately 30-40 solar occultation profiles per day, distributed across two latitude bands that precess over time due to the ISS orbital inclination.

In this study, we use SAGE III/ISS Version 6 aerosol extinction profiles at 355 nm, derived from the 384 nm channel and converted to 355 nm using the Ångström exponent computed from the 384-521 nm wavelength pair, for the period August 2024-April 2026. Prior to use, profiles were screened following the quality-control (QC) recommendations provided with the Level-2 product. Occultations affected by event-level anomalies, including pointing, blockage, timing, thermal-control, or ephemeris issues, were excluded, as were altitude bins flagged for signal disturbance or interpolation artefacts. For the aerosol comparisons, only measurements classified as background, perturbed, or enhanced aerosol by the SAGE aerosol classification

flag were retained; profiles flagged as transmission anomalies, aerosol-cloud mixtures, or polar stratospheric clouds were discarded. Finally, only positive extinction values with a relative uncertainty below 50 % were retained in the point-by-point comparison with ATLID. SAGE III/ISS constitutes the primary reference instrument for this validation study owing to its high measurement accuracy, self-calibrating nature, and the large number of collocations achievable with ATLID over the study period.

## 2.4 Ground-based lidar instruments

### 2.4.1 Table Mountain Facility (TMF)

The JPL (Jet Propulsion Laboratory) Table Mountain Facility (TMF; Leblanc et al. 2012; 34.38° N, 117.68° W, 2285 m a.s.l.) in California hosts the TMSOL (Table Mountain Stratospheric Ozone Lidar), operated by NASA's Jet Propulsion Laboratory within the NDACC network. Aerosol profiles are derived from nighttime-only, high-intensity UV Rayleigh (355 nm) and Raman (387 nm) lidar returns measured two to five times per week. The data are processed using the NDACC-compliant Global Lidar Analysis Software Suite (GLASS) v1 algorithm (Leblanc et al., 2016a, b), yielding aerosol backscatter and scattering ratio profiles at 355 nm normalised in an aerosol-free reference region between 32 and 36 km. The total uncertainty on the retrieved profiles is approximately 10 % throughout most of the stratosphere, with a vertical resolution ranging from a few tens of metres in the lowermost stratosphere to about 2.5 km in the upper stratosphere (Khaykin et al., 2026).

In this study, we use the standard NDACC aerosol backscatter coefficient product at 355 nm, screened according to the associated quality flags and averaged onto 2 km altitude layers. For the sAOD comparison (Sect. 3.3), TMF backscatter profiles are converted to extinction with a lidar ratio of 50 sr, while for the backscatter-based analysis (Sect. 3.5) we retain the native backscatter units and perform a direct comparison with ATLID L1 $\beta_{\mathrm{aer}}$.

### 2.4.2 Observatoire de Haute-Provence (OHP)

The Observatoire de Haute-Provence (OHP; 43.94° N, 5.71° E, 683 m a.s.l.), located in southern France and operated by LATMOS/IPSL within the NDACC network, has provided continuous stratospheric aerosol observations since the early 1990s using two independent lidar systems: LiO3S, operating at 355 nm, and LTA operating at 532 nm (Khaykin et al., 2017). In this study we use the LiO3S aerosol measurements at 355 nm, acquired at a mean rate of 10-12 nights per month (Godin-Beekmann et al., 2003; Khaykin et al., 2017). Vertical profiles of stratospheric aerosols are retrieved using the Sasano-Fernald inversion method, providing aerosol backscatter and extinction coefficients; the scattering ratio is computed as the ratio of total (molecular plus aerosol) to molecular backscatter, where the molecular contribution is derived from ECMWF meteorological analyses. The resulting profiles are reported at 150 m vertical resolution. A more detailed description of the instrument, retrieval methodology, and uncertainty budget is provided by Khaykin et al. (2017) and references therein.

OHP lidar data have previously been used for the validation of SAGE III/ISS aerosol extinction profiles (Knepp et al., 2020), demonstrating the suitability of this dataset as an independent stratospheric reference. In the present study, LiO3S backscatter profiles at 355 nm are treated identically to the TMF dataset and serve as an independent, ground-based validation reference

at a Northern Hemisphere mid-latitude site in a different longitude sector. For the sAOD comparison (Sect. 3.3), the thermal tropopause altitude is obtained from the ECMWF meteorological data provided with the L2A product, and backscatter profiles are converted to extinction using a lidar ratio of 50 sr; for the backscatter-based analysis (Sect. 3.5), we retain the native backscatter units and perform a direct comparison with ATLID L1 $\beta_{\mathrm{aer}}$.

### 2.5 Collocation methodology

ATLID and SAGE III/ISS profiles are collocated using the following criteria: a maximum spatial separation of 50 km, computed using the haversine formula between the SAGE III occultation tangent point and each individual ATLID footprint, and a maximum temporal difference of 12 h between the SAGE III occultation time and the ATLID overpass. For each SAGE III occultation satisfying these criteria, all ATLID Level-1 profiles falling within the collocation window are averaged together, and the resulting mean profile is interpolated onto the SAGE III vertical grid with 500 m step. ~~The exact time difference between each collocated ATLID mean profile and the corresponding~~ In the individual comparison figures, the distance (Dist) is the great-circle distance between the SAGE III/ISS tangent point and the closest of the averaged ATLID profiles, all of which lie within 50 km of the tangent point, and the time difference ($\Delta t$) is computed between the SAGE III~~occultation is recorded and displayed in the individual comparison figures~~/ISS event and each collocated ATLID overpass.

For ground-based lidar collocations, the same temporal criterion of 12 h is applied, with the spatial criterion adapted to the fixed station geometry: all ATLID overpasses occurring within a great-circle distance of 100 km from each lidar station are considered.

### 2.6 Comparison metrics

The agreement between ATLID and reference instruments is quantified using the ~~following metrics~~ metrics in Table 1, computed for the full collocation dataset.

**Table 1.** Comparison metrics used in this study to evaluate ATLID L1 and L2 extinction products against SAGE III/ISS and ground-based lidar.

| Metric | Definition and notes |
|---|---|
| Absolute bias | $\Delta\alpha(z) = \alpha_{\mathrm{ATLID}}(z) - \alpha_{\mathrm{ref}}(z)$, where $\alpha_{\mathrm{ref}}$ is the SAGE III/ISS or ground-based lidar extinction. |
| Relative bias | $\delta\alpha(z) = \Delta\alpha(z)/\alpha_{\mathrm{ref}}(z) \times 100\,\%$. Median differences are reported to characterize the distributions. |
| Std deviation | $\sigma_{\Delta\alpha}(z)$: standard deviation of $\Delta\alpha$ across the collocation ensemble at each altitude level. |
| Extinction scatter | Point-to-point comparison using 2D density histograms. Evaluated via linear regression (slope) and Pearson $R$. |
| sAOD | Stratospheric AOD integrated from the ATLID tropopause $+1$ km to 30 km. Compared via a 1:1 scatter diagram with linear regression fits. |
| Relative sAOD bias | $(\mathrm{sAOD}_{\mathrm{ATLID}} - \mathrm{sAOD}_{\mathrm{ref}})/\mathrm{sAOD}_{\mathrm{ref}} \times 100\,\%$. Evaluated as a function of latitude and time. |

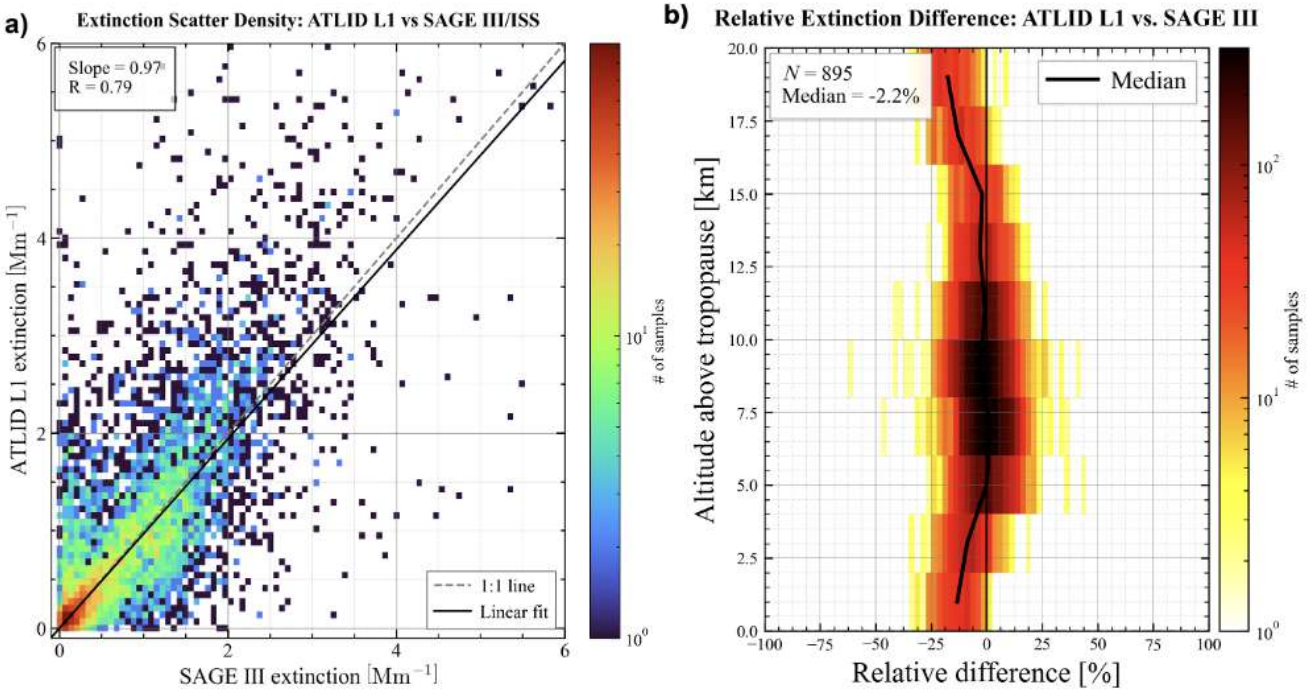



**Figure 1.** Comparison between ATLID L1 and SAGE III/ISS extinction coefficients. **a)** 2D density histogram for all collocated altitude-level pairs. The grey dashed line is the 1:1 reference; the solid black line is the ordinary least-squares linear regression (slope = 0.97, $R = 0.79$). **b)** Distribution of the relative difference as a function of altitude relative to the local tropopause, $z - z_{\mathrm{trop}}$ ($N = 895$ collocated profiles; see Sect. 2.5 for the definition of the collocation criteria); only levels at least 1 km above the local tropopause are included. The solid black line shows the ~~altitude-resolved~~ median ~~profile~~relative difference in each altitude bin; the thin vertical line marks zero relative difference. The overall median is ~~−2.3 %~~−2.2 %. For both panels, the colour scale gives the number of samples per bin on a logarithmic scale.

## 3 Results

The following subsections present the validation results in a logical sequence. We first establish the dataset characteristics (Sect. 3.1) and quantify the agreement between ATLID L1 and SAGE III/ISS at the profile level (Sect. 3.2) and in terms of integrated stratospheric AOD (Sect. 3.3). We then examine the spatio-temporal distribution of the relative sAOD bias (Sect. 3.4) and test the consistency of these findings against an independent ~~,~~comparison with ground-based backscatter observations at OHP and TMF (Sect. 3.5). Finally, we place the L1 results in context by demonstrating the limitations of the native Level-2 product across all aerosol regimes (Sect. 3.6).

Before presenting these results, we briefly summarise the limitations of the native ATLID L2 aerosol product in the stratosphere, which motivate the use of the L1-based extinction throughout this study. The L2 processor frequently returns zero extinction under background conditions; when it does return non-zero extinction in optically thicker layers, it overestimates the peak extinction (Sect. 3.2.2), and the resulting sAOD is only weakly correlated with the reference measurements (Sect. 3.6).

### 3.1 Overview of the collocation dataset

Over the study period from August 2024 to April 2026, the ATLID-SAGE III/ISS collocation procedure described in Sect. 2.5 produced a total of 895 co-located profile pairs, providing a statistically robust sample for the evaluation of ATLID performance across diverse atmospheric conditions. The number of co-located overpasses with the ground-based lidar stations is considerably smaller, reflecting the fixed-station geometry and the 25-day repeat cycle of EarthCARE: 55 events at TMF and 26 at OHP.

### 3.2 Altitude-resolved extinction comparison with SAGE III/ISS

The comparison between ATLID L1 and SAGE III/ISS extinction coefficients is presented in Fig. 1. Figure 1a displays all collocated altitude-level pairs as a 2D density histogram, in which the colour scale encodes the local sample count on a logarithmic scale. The bulk of the distribution is concentrated in the range 0-2 $\mathrm{Mm}^{-1}$, consistent with the dominance of near-background aerosol conditions in the dataset (Sect. 3.1). A linear regression through the full sample yields a slope of 0.97 and a correlation coefficient of $R = 0.79$, indicating a reasonably strong point-to-point correlation with a slight systematic underestimation of SAGE III/ISS extinction by ATLID L1 ($\sim$3 %). The scatter is substantial: a significant population of points lies well above the 1:1 line at low extinction (SAGE III/ISS $< 2\,\mathrm{Mm}^{-1}$)~~, consistent with the additive retrieval noise floor~~. This is expected from the random noise of the ATLID L1 extinction, which comes from the detection noise of the ATLID channels (in particular the Mie channels, whose signal is weak in the stratosphere) and whose absolute magnitude does not depend on the aerosol loading: a random error of roughly constant absolute magnitude produces a relative scatter that increases as the extinction decreases.

Figure 1b presents the distribution of the relative difference $(\alpha_{\mathrm{L1}} - \alpha_{\mathrm{SAGE}})/\alpha_{\mathrm{SAGE}}$ as a function of altitude relative to the local tropopause, $z - z_{\mathrm{trop}}$ (ATLID tropopause height; only levels at least 1 km above the tropopause are retained, consistent with the sAOD integration), for the full set of $N = 895$ collocated profiles (see Sect. 2.5). The overall median relative differ-

ence is ~~−2.3 %~~−2.2 %, confirming the near-zero systematic bias suggested by the regression slope in Fig. 1a and consistent with the near-unity sAOD regression reported in Sect. 3.3. The spread is large at all altitudes, with the distribution spanning approximately ±25 % between the 10th and 90th percentiles, reflecting the dominant contribution of retrieval noise to individual altitude-level comparisons under background conditions.

The ~~altitude~~ profile of the median bias (solid black line in Fig. 1b) reveals a distinct vertical structure. In the ~~lowermost stratosphere (approximately 10-13~~first ∼3 km ~~)~~above the tropopause, the median is ~~moderately positive (∼ +10 %), indicating that ATLID L1 slightly overestimates SAGE III/ISS extinction near the tropopause. Between approximately 13 and 17~~negative (about −10 to −15 %). Between about 5 and 15 km ~~, the median transitions sharply toward negative values, reaching its most negative excursion of approximately −15 % in the lower stratosphere. In the main aerosol layer (17-25 km), the median stabilises, indicating a consistent moderate underestimation by ATLID L1 throughout the bulk of the Junge layer. Above 25~~above the tropopause, it is close to zero, and it becomes negative again further up. Expressing the altitude relative to the local tropopause avoids mixing profiles with different tropopause heights; in geometric altitude, a small number of profiles with a low tropopause produced an apparent positive bias at 10-13 km~~, the median progressively approaches zero, consistent with both instruments approaching their respective noise floors as the aerosol signal weakens~~. The small overall median of ~~−2.3 % thus results from a partial cancellation between the positive near-tropopause contribution and the negative bias dominating the main aerosol layer; the underlying~~ −2.2 % therefore hides an altitude-dependent structure, discussed further in Sect. 4.1, ~~constitutes a~~ which is more physically meaningful ~~signature~~ than the single-number summary statistic.

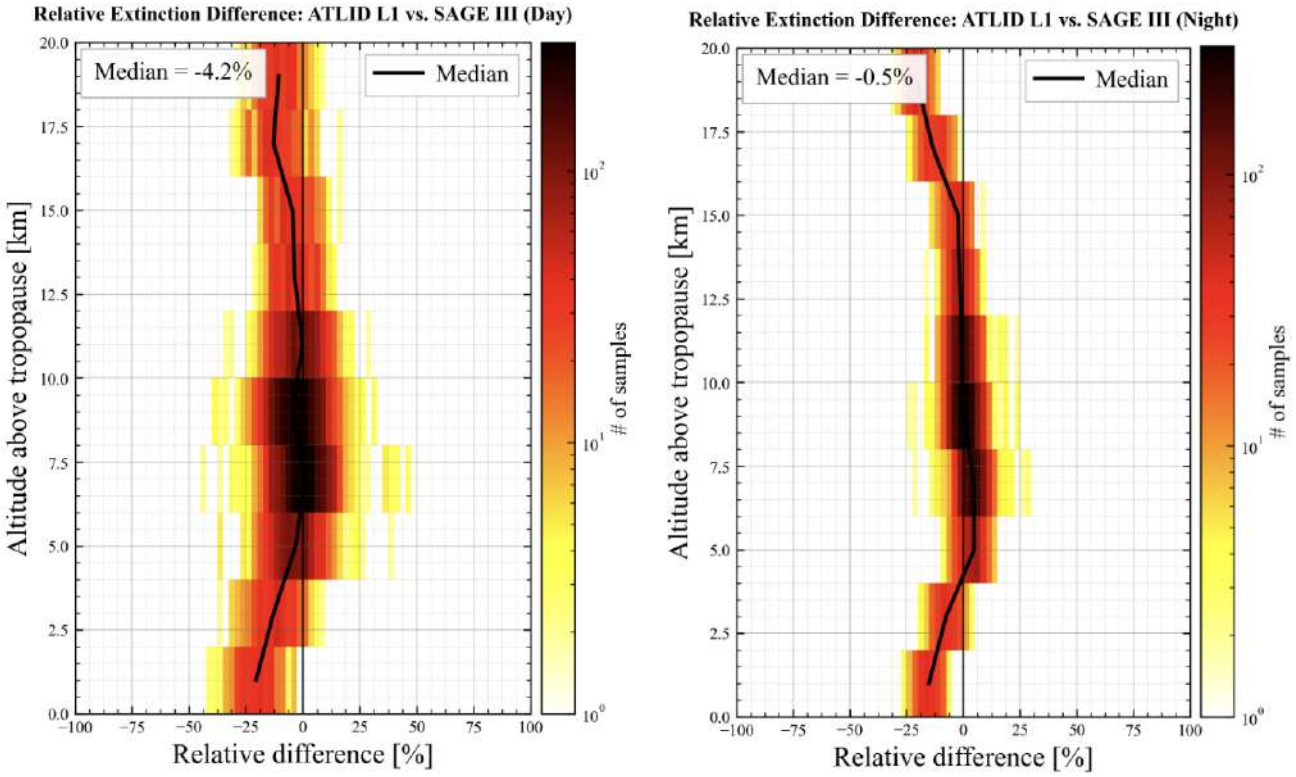



**Figure 2.** Relative extinction difference $(\alpha_{\mathrm{L1}} - \alpha_{\mathrm{SAGE}})/\alpha_{\mathrm{SAGE}}$ between ATLID L1 and SAGE III/ISS as a function of altitude above the local tropopause, shown separately for **(a)** daytime ATLID overpasses (SEA $> 0°$) and **(b)** nighttime ~~SAGE III/ISS occultations~~ATLID overpasses (SEA $\leq 0°$). The colour scale gives the number of samples per bin on a logarithmic scale. The solid black line shows the altitude-resolved median; the inset in each panel reports the overall median relative difference over the ~~12–30 km~~ displayed altitude range ($-4.2\,\%$ for daytime and $-0.5\,\%$ for nighttime).

### 3.2.1 Day-night dependence of the altitude-resolved bias

To assess whether the altitude-dependent bias structure identified above is affected by solar illumination, we separated the collocation ensemble ~~based on two independent daytime/nighttime criteria: the local solar time (LST) of the EarthCARE overpass, with 06:00 $\leq$ LST $\leq$ 18:00 classified as daytime and the remainder as nighttime; and the ATLID~~ according to the illumination conditions of the ATLID overpass, using the solar elevation angle (SEA) ~~at the collocation point (SEA~~of the collocated EarthCARE overpass: SEA $> 0°$ is classified as daytime ~~, SEA~~and SEA $\leq 0°$ as nighttime~~). Both criteria gave consistent classifications, and the~~ . This classification refers only to the ATLID observations; it does not separate sunrise and sunset SAGE III/ISS occultations, which are made under the same measurement geometry. The relative difference profiles were recomputed for each subset (Fig. 2). Both panels show 2D histograms of the relative difference $(\alpha_{\mathrm{L1}} - \alpha_{\mathrm{SAGE}})/\alpha_{\mathrm{SAGE}}$ as a function of altitude above the local tropopause.

The day and night subsets exhibit ~~remarkably~~ similar vertical structures~~. In both cases, ~~, as expected since this structure is mainly governed by factors common to both subsets, such as the vertical distribution of the aerosol loading and the altitude relative to the tropopause. In both cases,~~ the ~~median bias is slightly positive in the lowermost stratosphere (around 12-13 km), turns negative in the lower to middle stratosphere, and gradually returns toward zero above approximately 25 km, closely mirroring the behaviour~~ median relative difference follows the structure of the combined ensemble ~~in~~ (Fig. 1b~~. The main aerosol layer (17-25 km)is again characterised by a moderate negative bias of order −5 to −10 % for both day and night conditions~~), while the spread of the distribution remains ~~large~~ larger for the daytime subset at all altitudes~~, consistent with the dominant contribution of retrieval noise under near-background aerosol loading~~.

Quantitatively, the ~~vertically integrated~~ overall median bias differs only slightly between the two subsets, with values of ~~−4.6 %~~ −4.2 % for day and ~~−0.6 %~~ −0.5 % for night. ~~However, a~~ A more striking difference ~~between the two subsets~~ concerns the *spread* of the distribution: the ~~nighttime collocations~~ collocations with nighttime ATLID overpasses exhibit a substantially narrower dispersion at all altitudes ~~compared to daytime~~ than those with daytime overpasses, as is clearly visible in Fig. 2. ~~This is consistent with the well-known increase in SAGE III/ISS measurement noise during daytime occultations, which are affected by solar background radiation on the detector.~~ Quantitatively, the mean standard deviation of the relative differences, averaged over all altitude bins~~in the 12-30 km range~~, amounts to ∼32 % for the daytime subset and ∼17 % for the nighttime subset~~, confirming the improved signal-to-noise performance of nighttime occultations~~.

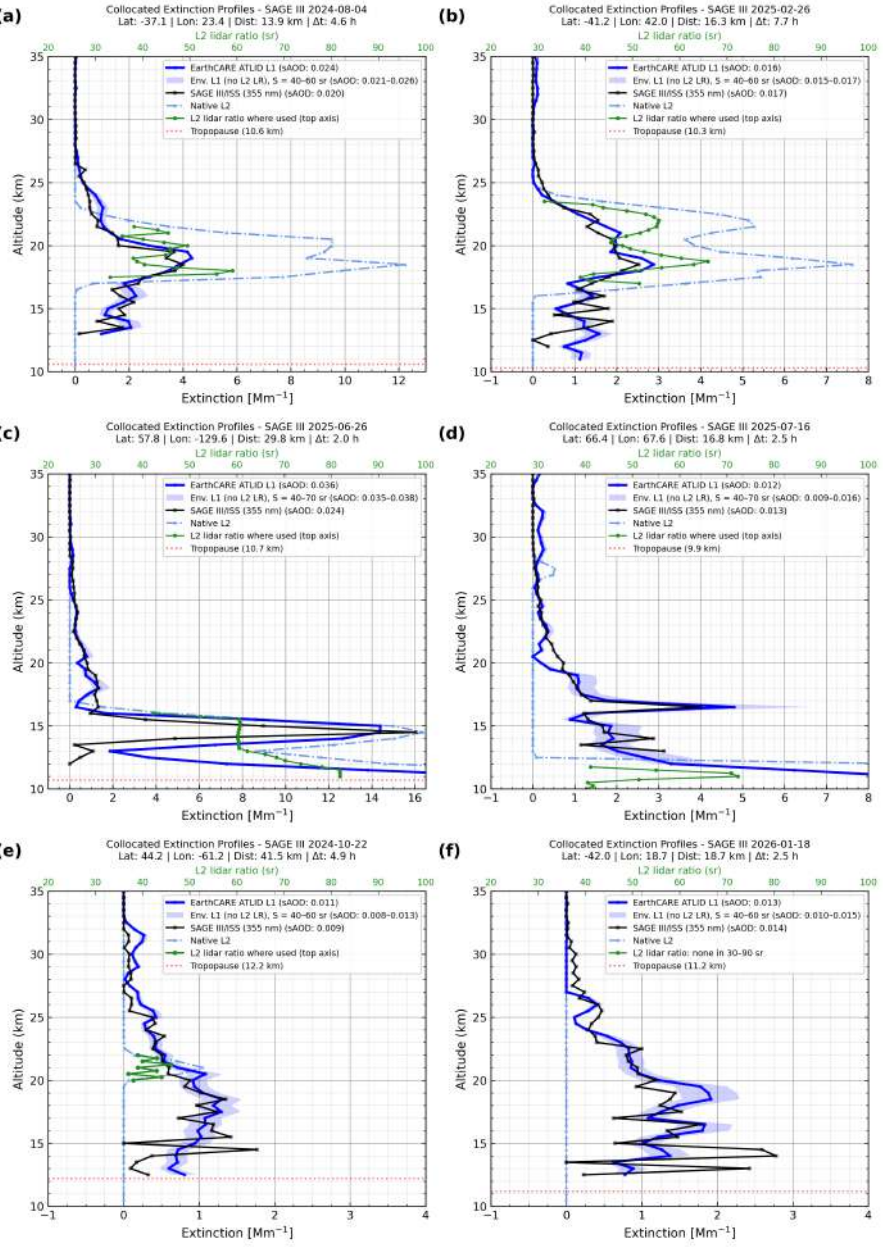



**Figure 3.** Collocated extinction profiles from SAGE III/ISS, ATLID L1 ~~,~~ and native ATLID L2~~for selected case studies.~~ : **(a, b)** ~~Southern Hemisphere~~ Ruang volcanic plume~~(older layer in b): L1 and SAGE III/ISS show coherent vertical structure~~, ~~while L2 overestimates the peak.~~ **(c, d)** ~~Boreal~~ boreal wildfire smoke~~: in the strong layer (c), residual L1/SAGE differences likely reflect plume spatial heterogeneity, and L2 again overestimates the peak; in the weaker layer~~ **(e, f)** background conditions. Green curve (~~d~~top axis)~~,~~ : L2 ~~misses~~ lidar ratio used in the ~~layer entirely.~~ **~~(e, f)~~** ~~Background conditions~~ L1 calculation (~~<~~ ~~2~~30-90 $Mm^{-1}$ sr). Blue envelopes: ~~L2 erroneously reports a narrow peak in place~~ L1 extinction for lidar ratios of ~~a diffuse layer in~~ 40-60 sr (~~e~~40-70 sr in c, d), shown only where no valid L2 lidar ratio is available. Dotted pink line: local tropopause. Dist: distance between the SAGE III/ISS tangent point and ~~returns zero extinction throughout in (f)~~the closest averaged ATLID profile; $\Delta t$: time difference between the SAGE III/ISS event and each ATLID overpass.

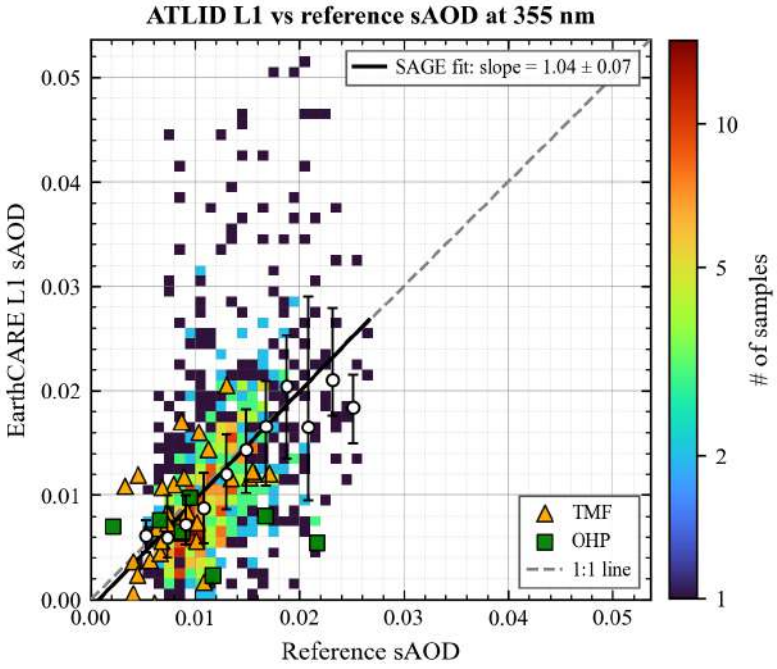



**Figure 4.** ~~Scatter diagram of~~ ATLID L1 sAOD versus reference sAOD, integrated from the ATLID-derived tropopause +1 km to 30 km. SAGE III/ISS matchups are shown as a 2D histogram (~~circles~~)number of matchups per 0.001 × 0.001 bin, logarithmic colour scale); TMF (triangles) ~~,~~and OHP (squares) matchups are shown individually. White circles give the median ATLID sAOD in 0.002-wide classes of SAGE III/ISS sAOD (classes with at least five matchups), ~~integrated from~~ with the ~~ATLID-derived tropopause +1 km to 30 km~~interquartile range as error bars. The dashed grey line is the 1:1 reference. The solid ~~blue~~ black line shows the linear regression fit to the SAGE III/ISS matchups: slope = $1.04 \pm 0.07$ ($\pm 1$ standard error), intercept = $(-0.8 \pm 0.9) \times 10^{-3}$, $R = 0.67$; the slope is also given in the upper-right corner.

The small day-night offset in median bias is well within the altitude-to-altitude variability of the median profiles of the relative difference (black lines in Fig. 2) and considerably smaller than the typical percentile spread at a given height, indicating that the ATLID L1 vs SAGE III/ISS extinction bias is, to first order, insensitive to the ~~solar~~ illumination conditions at the time of the ATLID overpass. ~~We therefore attribute the modest day-night differences primarily to changes in the signal-to-noise characteristics of the SAGE~~The larger dispersion of the collocations with daytime ATLID overpasses cannot be explained by the type of SAGE III/ISS ~~solar occultationmeasurements themselves rather than to any systematic~~ occultation: our day/night split does not separate sunrise and sunset events, and analyses by the SAGE III/ISS validation team show no appreciable difference between sunrise and sunset retrievals, either in comparisons with OHP or in zonal statistics over the period of this study (Anonymous Referee #1, 2026). We therefore do not attribute this difference to either instrument. Comparing daily zonal statistics of daytime and nighttime ATLID observations would be an appropriate way to quantify a possible illumination dependence of the ATLID L1 retrieval ~~on illumination conditions~~and is left for future work.

### 3.2.2 Representative profile case studies

Figure 3 presents six representative collocation case studies selected to illustrate the three distinct stratospheric aerosol regimes sampled in this study: volcanic plumes, wildfire smoke, and low aerosol background conditions. In each panel, the ATLID L1 profile (solid blue line) and the native ATLID L2 retrieval (~~dashed~~ dash-dotted light blue line) are compared against the SAGE III/ISS reference (solid black line); the local tropopause altitude is indicated by a horizontal ~~pink dashed line.~~ dotted pink line. The green curve (top axis) shows the L2 lidar ratio used in the L1 calculation, at the levels where it lies within 30-90 sr, and the blue envelope shows the L1 extinction obtained with lidar ratios of 40-60 sr (40-70 sr for the smoke cases) at the levels where the 50 sr fallback is used. Comparing these diverse scenes highlights the contrasting behaviour of the ATLID L1 and native L2 extinction products under varying aerosol loadings.

Panels (a) and (b) correspond to Southern Hemisphere collocations affected by the Ruang volcanic plume, acquired on 4 August 2024 (lat ~~$-37.1°, \Delta t = 6.7$~~ $= -37.1°$, $\Delta t = 4.6$ h) and 26 February 2025 (lat ~~$-41.2°, \Delta t = 3.8$~~ $= -41.2°$, $\Delta t = 7.7$ h), respectively. In both cases, ATLID L1 and SAGE III/ISS reproduce a coherent vertical structure with a pronounced extinction peak in the ~~14-18~~16-22 km range, consistent with the known altitude of the volcanic injection layer after its poleward transport (K26). The native L2 product systematically overestimates the peak extinction in both panels, yielding values up to a factor of ∼2-3 above the SAGE III/ISS reference.

Panels (c) and (d) show collocations within boreal wildfire smoke layers, acquired on 26 June 2025 (lat ~~$57.8°, \Delta t = 0.3$~~ $= 57.8°$, $\Delta t = 2.0$ h) and 16 July 2025 (lat ~~$66.4°, \Delta t = 5.6$~~ $= 66.4°$, $\Delta t = 2.5$ h), respectively. The stronger layer in panel (c) (ATLID L1 sAOD ~~$= 0.031$~~ $= 0.036$) is well captured by both ATLID L1 and SAGE III/ISS, with a sharp extinction peak near ~~12-14~~12-16 km reaching approximately 8-16 $\mathrm{Mm}^{-1}$; residual differences between L1 and SAGE III/ISS at the peak are likely attributable to the spatial heterogeneity of the smoke plume given the ∼30 km collocation distance, rather than to a systematic retrieval error. The L2 product again overestimates the peak extinction in panel (c). In this case, the L2 provides a lidar ratio of about 60 sr within the smoke layer, which is used in the L1-derived extinction; the L1 sAOD (0.036) is then higher than the SAGE III/ISS sAOD (0.024). In the weaker companion layer of panel (d) (SAGE III/ISS sAOD = 0.013), ATLID L1 and SAGE III/ISS remain in reasonable agreement across the stratospheric column (L1 sAOD = 0.012, or 0.009-0.016 for lidar ratios of 40-70 sr), while the native L2 product fails to detect the layer~~entirely~~, returning near-zero extinction throughout the ~~profile~~smoke layer (13-20 km); no valid L2 lidar ratio is available there, and the 50 sr fallback is used.

Panels (e) and (f) represent background conditions with stratospheric aerosol optical depths below approximately 0.015, acquired on 22 October 2024 (lat ~~$44.2°, \Delta t = 1.0$~~ $= 44.2°$, $\Delta t = 4.9$ h) and 18 January 2026 (lat ~~$-42.0°, \Delta t = 8.3$~~ $= -42.0°$, $\Delta t = 2.5$ h), respectively. Under these low-loading conditions, ATLID L1 and SAGE III/ISS consistently show a diffuse, weakly structured extinction profile with values below ∼2 $\mathrm{Mm}^{-1}$ throughout the stratospheric column. The L2 retrieval fails in qualitatively different ways in each case: in panel (e), it ~~produces a spurious, narrow extinction peak near 13~~detects only a thin layer near 20-22 km ~~with no counterpart in either the~~ within the diffuse layer seen by ATLID L1 ~~or~~ and SAGE III/ISS~~profiles~~, and returns zero extinction elsewhere; in panel (f), it returns strictly zero extinction across the entire stratospheric column, representing a complete retrieval failure. Consequently, a valid L2 lidar ratio (about 35-45 sr) is available in panel (e) only

around 20-22 km, and the 50 sr fallback is used elsewhere, whereas in panel (f) no valid L2 lidar ratio is available and the fallback is used throughout the profile. Together, these six case studies demonstrate that the skill of the native ATLID L2 stratospheric aerosol retrieval degrades markedly with decreasing aerosol loading, while the L1-based K26 product maintains consistent agreement with SAGE III/ISS across all regimes, providing a clear rationale for its use as the primary extinction estimate throughout the remainder of this study.

### 3.3 Stratospheric AOD comparison

Figure 4 ~~presents the scatter diagram of~~ compares the ATLID L1 sAOD ~~against~~ with the reference sAOD from SAGE II-I/ISS and the available ground-based lidar stations (TMF, OHP), integrated from the ATLID tropopause $+1$ km to 30 km. For SAGE III/ISS, the sAOD is computed by integrating the extinction profiles over the same altitude range; the stratospheric_aerosol_optical_d parameter of the SAGE III/ISS Level-2 product is not used. Reference sAOD values span approximately 0-0.030 for the SAGE III/ISS matchups, covering background conditions, the volcanic perturbation associated with the Ruang eruption (April-May 2024), and the wildfire smoke events of boreal summer 2025.

A linear regression applied to the SAGE III/ISS matchups yields a slope of $1.04 \pm 0.07$, an intercept of $(-0.8 \pm 0.9) \times 10^{-3}$ ($R = 0.67$), indicating that the ATLID L1 product is, on average, essentially unbiased with respect to SAGE III/ISS integrated sAOD. However, the scatter around the regression line is not uniform across the dynamic range and reveals contrasting behaviour between the low- and high-aerosol-loading regimes. While the dense core of the data remains broadly consistent with the 1:1 line, the high-loading regime (reference sAOD $> 0.010$) exhibits an asymmetric dispersion. Specifically, there is a prominent subset of ATLID L1 retrievals that yield significantly higher values than the SAGE III/ISS reference, creating a pronounced positive tail in the distribution.

The class medians of Fig. 4 (white circles) show how the agreement varies with the aerosol loading. Above about 0.02, few matchups remain and the interquartile range widens.

Two factors may contribute to the positive tail at high aerosol loading. (i) Coverage of the lowermost stratosphere: both sAODs are integrated from the tropopause $+1$ km to 30 km, but in dense layers the lowest SAGE III/ISS levels are more likely to be removed by the quality screening (e.g. aerosol-cloud mixture flag) or not retrieved at all, as the transmission along the line of sight decreases, whereas the ATLID L1 profile retains these levels. When a dense layer lies just above the tropopause, as in Fig. 3c, where ATLID shows large extinction values between the tropopause and 12.5 km that are absent from the SAGE III/ISS profile, the ATLID sAOD therefore includes a contribution that is missing from the SAGE III/ISS sAOD. (ii) Sampling geometry: SAGE III/ISS integrates along a limb path of a few hundred kilometres, whereas the ATLID extinction is an average of nadir profiles within 50 km. For compact plumes, ATLID can sample the core of the plume while SAGE III/ISS sees it diluted along its line of sight, which produces large positive differences; in the opposite case, the negative difference is limited by this dilution. This favours a positive tail at high aerosol loading.

Among the ground-based reference instruments, the TMF matchups (orange triangles) scatter on both sides of the 1:1 line without a clear directional offset, broadly mirroring the noise-dominated behaviour of the SAGE III/ISS ensemble at comparable sAOD levels. The OHP matchups (green squares) follow the same qualitative low-/ high-loading pattern, with

a tendency for points to fall below the 1:1 line as the reference sAOD increases; more matchups lie below than above the regression line overall, foreshadowing the systematic negative offset identified independently for this station from the point-to-point backscatter comparison in Sect. 3.5. For these sAOD comparisons, the ground-based backscatter profiles are converted to extinction with a lidar ratio of 50 sr (Sect. 2.4), while the ATLID L2 lidar ratio is used only where it lies within 30-90 sr and 50 sr is used elsewhere, so the two conversions differ only at these levels. The backscatter comparison of Sect. 3.5 is independent of the lidar ratio.

### 3.4 Latitudinal and temporal distribution of the relative sAOD bias

Figure 5 presents the relative sAOD difference $(\mathrm{sAOD_{L1}} - \mathrm{sAOD_{ref}})/\mathrm{sAOD_{ref}}$ as a function of latitude (panel a) and time (panel b) for the SAGE III/ISS, TMF, and OHP matchups. Across all matchups, the relative sAOD bias has a global mean of $-3.2\,\%$ with a standard deviation of $65.7\,\%$, indicating a near-zero systematic offset combined with a large point-to-point scatter.

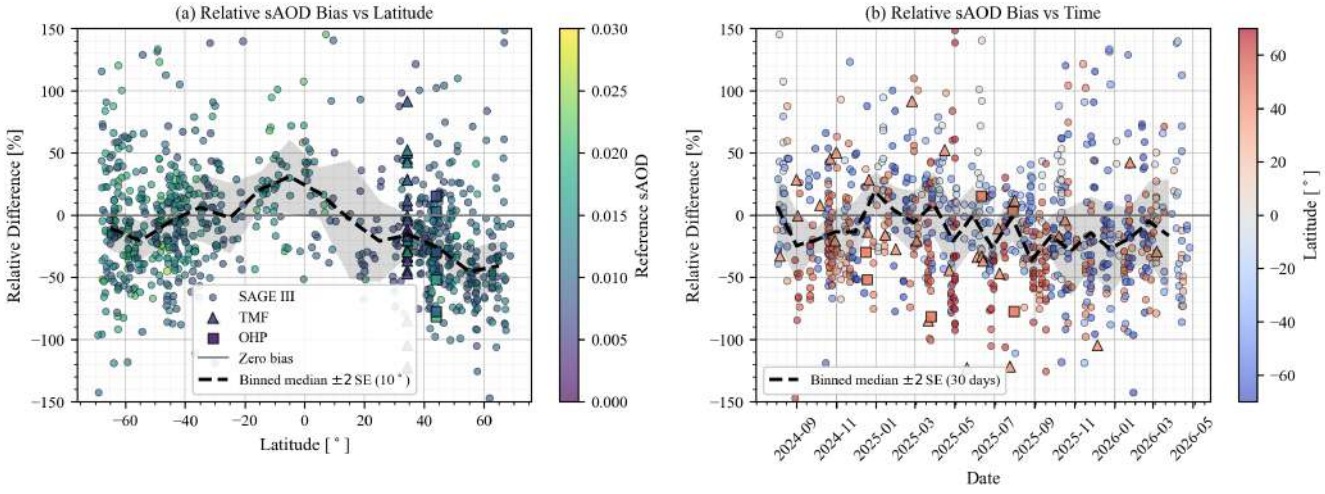



**Figure 5.** Relative sAOD bias of ATLID L1 with respect to SAGE III/ISS (circles), TMF (triangles), and OHP (squares) as a function of (a) latitude and (b) time. Symbol colours encode the reference sAOD in panel (a) and the collocation latitude in panel (b). The solid grey line marks zero bias; the dashed black line is the binned median relative difference (10° latitude bins in panel a, 30-day windows in panel b), and the surrounding grey shaded envelope shows its ±2 standard-error (±2 SE) interval, i.e. an approximate 95 % confidence range on the median in each bin.

The latitudinal distribution (Fig. 5a) reveals a clear meridional gradient in the SAGE III/ISS-based comparisons, with ATLID L1 exhibiting a systematic negative bias in the Northern Hemisphere extratropics that increases with latitude. The grey shaded envelope around the dashed line represents the ±2 standard-error (±2 SE) interval of the binned median, i.e. an approximate 95 % confidence range in each bin; it is ~~narrow~~ narrowest where collocations are dense (~~the tropics and NH~~ mid-latitudes) and ~~broad in the sparsely sampled polar bins~~broadest where they are sparse, in particular in the Northern Hemisphere

tropics and subtropics (10-30° N), providing a visual guide to which median excursions are statistically robust rather than an artefact of limited sampling. The scatter is large at all latitudes, with individual relative differences frequently exceeding $\pm 50\,\%$, consistent with the standard deviation reported above. Among the ground-based stations, the TMF matchups (triangles, $34^\circ$ N) span a wide range of both positive and negative relative biases, while the OHP matchups (squares, $44^\circ$ N), though limited in number, are predominantly negative, consistent with the tendency noted in Sect. 3.3 and confirmed independently in Sect. 3.5.

The temporal distribution (Fig. 5b) shows no obvious secular drift over the 20-month record, indicating broad stability of the ATLID L1 calibration throughout the study period. The apparent see-saw pattern of the 30-day binned median likely reflects the changing latitudinal sampling of SAGE III/ISS, with intervals dominated by Northern Hemisphere extratropical matchups showing a more negative bias, consistent with the low bias identified for NH mid- to high-latitude comparisons in Fig. 5a, rather than any systematic temporal drift of the ATLID L1 product. The $\pm 2$ SE envelope on the median widens during intervals with fewer collocations, and no monotonic trend emerges beyond this envelope, reinforcing the absence of a significant temporal drift and the broad stability of the ATLID L1 calibration.

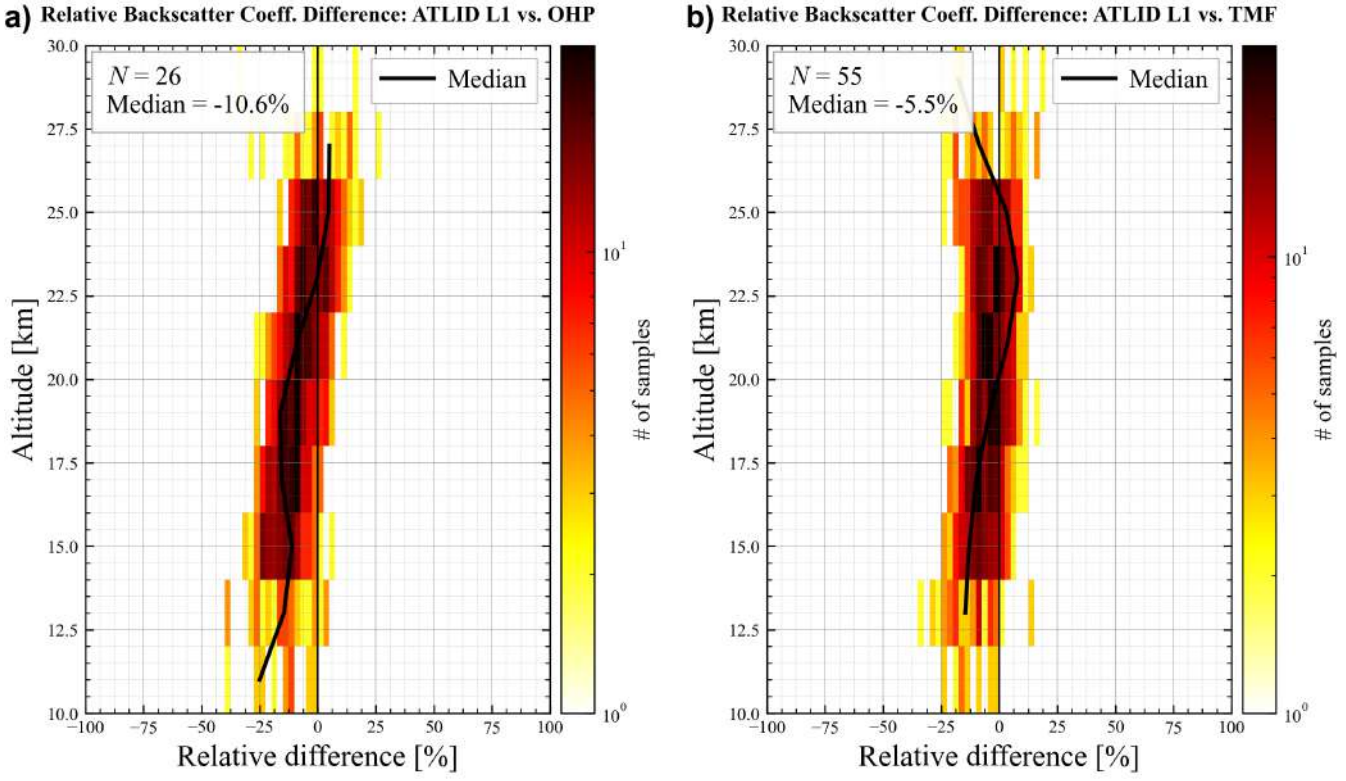



**Figure 6.** Distribution of the relative difference between ATLID L1 and ground-based lidar particulate backscatter coefficients as a function of altitude for **(a)** OHP ($N = 26$ collocated overpasses) and **(b)** TMF ($N = 55$ collocated overpasses). In each panel, the colour scale gives the number of samples per bin on a logarithmic scale. The solid black line shows the altitude-resolved median profile; the thin vertical line marks zero relative difference. The overall median relative differences are $-10.6\,\%$ (OHP) and $-5.5\,\%$ (TMF).

### 3.5 Point-to-point backscatter coefficient comparison: OHP and TMF

The comparisons presented above rely, to varying degrees, on the conversion from ATLID L1 backscatter to extinction via a lidar ratio (Eq. (1)). This lidar ratio is taken from the ATLID L2 product when ~~available~~it is available and lies within 30-90 sr, and set to a fixed value of 50 sr otherwise (see Sect. 2.2). To isolate the contribution of this conversion step from that of the underlying scattering-ratio retrieval, we additionally compare ATLID L1 particulate backscatter coefficients directly against collocated ground-based lidar backscatter profiles at OHP and TMF, applying the same point-to-point relative-difference metric defined in Sect. 2.6 but evaluated on $\beta_{\mathrm{aer}}$ rather than on extinction.

Figure 6 shows the resulting distributions of the relative backscatter difference as a function of altitude for the $N = 26$ OHP overpasses (panel a) and the $N = 55$ TMF overpasses (panel b). At OHP, the overall median relative difference is $-10.6\,\%$, while at TMF it amounts to $-5.5\,\%$. Both values are negative, confirming a systematic tendency for ATLID L1 to underestimate ground-based backscatter, consistent with the underestimation identified in the SAGE III/ISS extinction comparison (Sect. 3.2). The difference in magnitude between the two stations (OHP exhibiting a roughly twice as large negative offset as TMF) may

reflect the smaller OHP sample size, differences in the altitude ranges effectively sampled by each lidar, or a genuine site-dependent component.

Interestingly, both lidar stations confirm a slight negative bias in the lower stratosphere just above the tropopause, consistent with the behaviour found in the SAGE III/ISS comparison in tropopause-relative altitude (Fig. 1b). The scatter of the differences is also similar to that observed for the ~~nighttime SAGE III/ISS collocations , as all lidar collocations are nighttime observations~~collocations with nighttime ATLID overpasses (Sect. 3.2.1). The OHP profile displays a similar structure, with the negative bias concentrated between 11 and 23 km and a clearer positive excursion near 23-27 km. Because both comparisons are, by construction, independent of the lidar ratio, this three-instrument consistency strongly indicates that the altitude-dependent bias structure identified throughout Sect. 3.2 originates predominantly in the Level-1 scattering-ratio retrieval itself, rather than in the extinction-conversion step (Sect. 2.2).

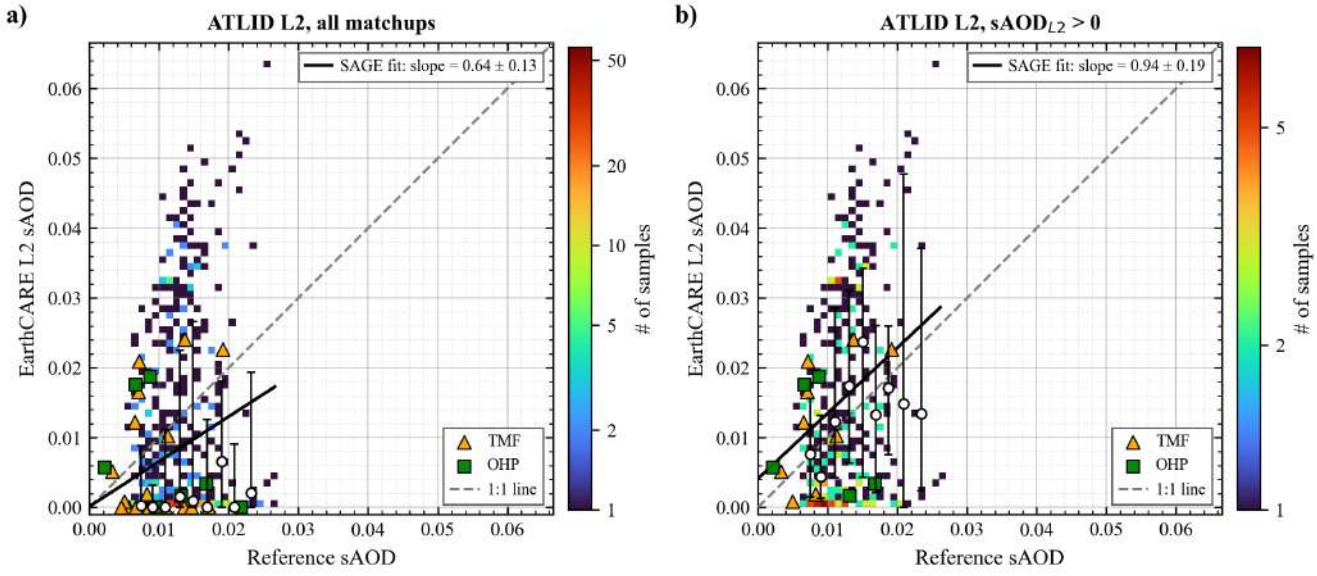



**Figure 7.** ~~Scatter diagrams of~~ Same as Fig. 4, but for the native ATLID L2 sAOD~~versus reference sAOD from SAGE III/ISS (circles), TMF (triangles), and OHP (squares), integrated from the ATLID-derived tropopause + 1 km to 30 km~~. **(a)** All ~~collocated~~ matchups, including ~~cases for which the~~ those with zero L2 ~~processor returns no stratospheric retrieval~~ extinction at all levels ($sAOD_{L2} = 0$, ~~visible along the horizontal axis~~bottom row). ~~The linear regression fit~~ Fit to the SAGE III/ISS matchups ($N = 652$)~~yields a~~ : slope~~of $0.64 \pm 0.13$ and an~~ $= 0.64 \pm 0.13$, intercept~~of $(0.1 \pm 1.7) \times 10^{-3}$ (~~ $= (0.1 \pm 1.7) \times 10^{-3}$, $R = 0.19$~~)~~. **(b)** ~~Same comparison but restricted to actual retrievals ($sAOD_{L2} > 0$); the null retrievals ($sAOD_{L2} = 0$) shown along the horizontal axis in panel (a) are here excluded from both the display and the fit. The regression to the SAGE III/ISS~~ Only matchups with $sAOD_{L2} > 0$ ($N = 331$)~~then yields a~~ : slope~~of $0.94 \pm 0.19$ with a positive~~ $= 0.94 \pm 0.19$, intercept~~of $(4.1 \pm 2.6) \times 10^{-3}$ (~~ $= (4.1 \pm 2.6) \times 10^{-3}$, $R = 0.26$~~)~~. ~~In both panels,~~ There are fewer matchups than in Fig. 4 because the ~~dashed grey line is~~ daily L2 files contain fewer profiles than the ~~1:1 reference and quoted uncertainties are one standard error~~L1 files (about 6400 vs. 22 750 per day).

### 3.6 Rationale for the Level-1-based retrieval: comparison with native Level-2 products

Having established the robustness of the Level-1-based (K26) extinction product across diverse stratospheric conditions, we now evaluate the added value of this approach relative to the native ATLID Level-2 (L2) aerosol retrieval. Figure 7a ~~shows the scatter of~~ compares the L2 stratospheric AOD ~~against~~ with the reference sAOD from SAGE III/ISS, TMF, and OHP. A linear regression to the SAGE III/ISS matchups yields a slope of only 0.64 and an intercept of $0.1 \times 10^{-3}$, well below the near-unity slope obtained for the L1 product ~~over the same matchup ensemble~~ (slope $= 1.04 \pm 0.07$, intercept $= (-0.8 \pm 0.9) \times 10^{-3}$; Sect. 3.3, Fig. 4). ~~The~~ In about half of the matchups (321 of 652), the L2 ~~product is also visibly sparser than the L1 product in~~ extinction is zero at all levels of the integration range ($\mathrm{sAOD_{L2}} = 0$, bottom row of Fig. 7a), reflecting the frequent ~~occurrence of fill values~~ absence of aerosol detection by the L2 processor noted in Sect. 2.2. These zeros are reported by the L2 product itself and are used as such in the sAOD integration, while true fill values are discarded. The L2 comparison also includes fewer matchups than the L1 comparison (652 vs. 895) because the daily L2 files contain fewer profiles than the L1 files (about 6400 vs. 22 750 per day).

Restricting the comparison to profiles for which the L2 processor returns an actual stratospheric retrieval ($\mathrm{sAOD_{L2}} > 0$; Fig. 7b) partially compensates for the systematic underestimation seen in panel (a): the SAGE III/ISS regression slope rises from $0.64 \pm 0.13$ to $0.94 \pm 0.19$, formally consistent with unity. This improvement is, however, largely artificial. It results from the removal of the numerous null retrievals ($\mathrm{sAOD_{L2}} = 0$) that pull the full-sample slope downward, rather than from any genuine skill of the L2 product. Indeed, the correlation remains very weak ($R = 0.26$) and the fit acquires a significantly positive intercept of $(4.1 \pm 2.6) \times 10^{-3}$, indicating that the retained L2 retrievals scatter almost independently of the true aerosol loading and, on average, overestimate the low-sAOD background. Even when the L2 processor does converge to a non-zero solution, the resulting sAOD is therefore only loosely tied to the reference value, and the apparent near-unity slope in panel (b) should not be interpreted as evidence of reliable quantitative agreement. The class medians confirm this picture: because about half of the matchups have $\mathrm{sAOD_{L2}} = 0$, they stay close to zero over most of the sAOD range in Fig. 7a, and when these cases are excluded (Fig. 7b), they fall on both sides of the 1:1 line with wide interquartile ranges, so that no sAOD range of consistent agreement emerges.

At low reference sAOD ($\lesssim 0.02$), where the bulk of the dataset lies, L2 retrievals show essentially no relationship with the reference values: some matchups return spuriously high sAOD (up to 0.05-0.06) while others return values close to zero, regardless of the true aerosol loading. This behaviour is illustrated at the profile level by the selected case studies shown in Fig. 3, spanning the three aerosol regimes sampled in this study. Taken together, the aggregate sAOD comparison and the case-level profiles demonstrate that the skill of the native L2 retrieval degrades sharply as the aerosol loading decreases, and justify the systematic use of the L1-based K26 product as the primary ATLID extinction estimate throughout the remainder of this study.

## 4 Discussion

We now discuss the possible physical origins of the bias patterns identified in Sect. 3, the practical implications of the L1/L2 contrast for ATLID data users, and the main limitations of the present analysis.

### 4.1 Altitude/Latitude-dependent structure of the ATLID bias

The altitude-dependent bias identified independently in the SAGE III/ISS extinction comparison (Sect. 3.2) and in the OHP and TMF backscatter comparisons (Sect. 3.5) is ~~mainly~~ consistent across the three instruments ~~: all three agree in the lower-to-mid stratosphere, whereas~~ near the tropopause~~the sign of the bias differs between SAGE III/ISS and the ground-based lidars, with a positive bias for SAGE III/ISS. These features point toward a small number of plausible physical origins.~~

~~The positive offset near the tropopause is specific to the SAGE~~: when expressed as a function of altitude above the local tropopause, the SAGE III/ISS comparison ~~: OHP and TMF both remain negative at the same altitudes rather than showing a comparable positive excursion (Sect. 3.5), which argues against a reference-independent artefact such as genuine cloud contamination of the ATLID profiles and instead points to a SAGE-specific factor, for instance, differences in effective tropopause altitude or the explicit SAGE III/ISS screening of aerosol-cloud mixtures near the tropopause (Sect. 2.3). The pronounced negative excursion through the lower-to-mid stratosphere, by contrast, is common to SAGE III/ISS, OHP, and TMF alike; while this consistency~~ shows a negative bias just above the tropopause, as do the two ground-based lidars.

This consistency between the lidar-ratio-dependent extinction comparison and the lidar-ratio-independent backscatter comparisons argues against the conversion step being the dominant driver and instead points to an origin within the Level-1 scattering-ratio retrieval itself~~,~~ ; the exact physical mechanisms driving this ~~distinct~~ vertical bias structure require further investigation. ~~Above ~25 km, the convergence of both comparisons toward near-zero bias is most plausibly explained by both instruments approaching their respective noise floors as the aerosol signal weakens.~~

This behaviour is broadly consistent with the lessons learned from the CALIOP stratospheric aerosol product. Kar et al. (2019) showed that the improved Version 4 calibration of CALIOP enabled a reliable retrieval of stratospheric aerosol extinction, but also that agreement with SAGE III/ISS remains strongly latitude- and altitude-dependent: comparatively good in the tropical stratosphere between about 20 and 30 km, and substantially poorer at higher latitudes and near the tropopause, where differences can exceed 100 %. Those results are particularly relevant here because they show that, even for a mature elastic lidar product, the stratospheric regime remains challenging when the aerosol loading is weak and the signal-to-noise ratio is low.

ATLID itself exhibits an analogous latitudinal signature: the sAOD bias distribution (Sect. 3.4, Fig. 5a) shows a systematic negative bias in the Northern Hemisphere extratropics that increases with latitude. Part of this gradient may be linked to aerosol type rather than to latitude *per se*: the boreal wildfire smoke events sampled during this study are concentrated at Northern Hemisphere mid-to-high latitudes, and ~~smoke particles are expected to depart more strongly from the fixed~~ the lidar ratio of smoke particles may differ from the 50 sr ~~lidar ratio~~ fallback used in the absence of a valid L2 value (Sect. 2.2)~~than aged background sulfate aerosol~~. The case studies of Fig. 3 show, however, that this effect alone cannot explain the negative

bias: in the smoke case of Fig. 3c, the L2 provides a lidar ratio of about 60 sr within the layer and the L1 sAOD exceeds the SAGE III/ISS value, while in Fig. 3d the L1 sAOD obtained with the 50 sr fallback is close to the SAGE III/ISS value. The lidar ratio of smoke is therefore only one possible contribution, and a dedicated analysis comparing the summer 2025 smoke period with the rest of the record is left for future work.

To further contextualize the degree of agreement observed between ATLID L1 and SAGE III/ISS, it is instructive to compare our results with other satellite intercomparison studies. For instance, Kovilakam et al. (2023) evaluated the consistency between SAGE III/ISS extinction and CALIOP backscatter-derived extinction (see their Fig. 13). They demonstrated that direct comparisons using a constant lidar ratio for CALIOP yielded regional biases frequently exceeding 50 % in the lower stratosphere and at higher latitudes. It was only after applying an empirical, altitude- and latitude-dependent scale factor to the CALIOP data that the differences relative to SAGE III/ISS were reduced to within $\pm 20$ %. In this context, the agreement found in our study without relying on any empirical post-scaling highlights the robust performance of the ATLID L1-based retrieval and the distinct advantage of its HSRL measurement capabilities in the stratosphere.

### 4.2 Implications of the Level-1/Level-2 contrast for data users

The clear contrast between the regression slopes obtained for the L1 (1.04) and native L2 (0.64) sAOD products against SAGE III/ISS (Sect. 3.6) has direct practical implications. The native L2 stratospheric aerosol product, in its current processing baseline, should not be relied upon for quantitative assessments of background or weakly perturbed stratospheric aerosol, the regime that dominates the EarthCARE record outside of the Ruang eruption and the 2025 boreal wildfire season, since it exhibits essentially no skill in this regime and frequently defaults to either spuriously elevated or null retrievals. The L1-based K26 product evaluated throughout this study provides a substantially more faithful representation of the true aerosol loading across the full dynamic range sampled here, and we recommend its use, at least in the interim, for stratospheric aerosol monitoring and trend studies based on ATLID, pending future refinement of the operational L2 algorithm.

The quality of the SAGE III/ISS reference data is also important in interpreting these comparisons. The extinction profiles used here are derived from the 384 nm channel and converted to 355 nm using the 384-521 nm Ångström exponent, with profiles affected by transmission anomalies, cloud contamination, or large fractional uncertainty excluded following established quality-control recommendations (Knepp et al., 2020). Using the 384/449 nm pair instead (mean Ångström exponent of 0.704 over the ATLID observation period, compared with 0.866 for the 384/521 nm pair) would change the 384-to-355 nm conversion factor from 1.070 to 1.057, i.e. the converted 355 nm extinction by only about 1.3 %, which is small compared with the variability and uncertainties of the ATLID-SAGE III/ISS comparison. SAGE III/ISS is therefore a robust and well-characterized reference, but not a noise-free one; some of the residual scatter in the ATLID comparison likely reflects the combined uncertainties of both instruments.

Beyond the reference dataset itself, the extinction retrieval relies on a lidar ratio that is either taken from the ATLID L2 product~~or, when unavailable,~~ , where it lies within 30-90 sr, or fixed at 50 sr ~~regardless of aerosol type~~ otherwise (Sect. 2.2). ~~Although assuming a fixed lidar ratio is a theoretical source of uncertainty, it is unlikely to introduce a significant systematic bias in our dataset. For optically thick, fresh plumes (such as dense volcanic ash or absorbing wildfire smoke), the ATLID L2~~

processor generally provides reliable, directly measured lidar ratios that supersede the fallback. Conversely, for aged plumes and For aged plumes and near-background stratospheric conditions where the stratospheric conditions, where the L2 retrieval defaults to fill values , the true physical lidar ratiois expected to be close to product reports zero extinction, the 50 sr value is an assumption. Typical lidar ratios of stratospheric sulfate are about 45-50 sr at 532 nm (Kremser et al., 2016), but direct estimates at 355 nm are scarce: Vaughan et al. (2021) used 40-50 sr at 355 nm for the 2019 Raikoke and Ulawun sulfate layer, checked against Raman measurements, and a constant 50 sr is used for sulfate aerosol with the 355 nm LiO3S lidar at Maïdo (K26). The 50 sr value thus lies at the upper end of the values used at 355 nm. Since the L1-derived extinction scales linearly with the lidar ratio, a $\pm 10$ sr departure from 50 sr changes the extinction by $\pm 20\,\%$; this sensitivity is shown as an envelope in Fig. 3 at the levels where the 50 sr assumed value. A full quantitative sensitivity analysis is left for future work, including a fallback is used. A targeted test of the smoke-related, high-latitude hypothesis raised in Sect. 4.1 is left for future work. We note, however, that the qualitative consistency between the lidar-ratio-dependent SAGE III/ISS extinction comparison and the lidar-ratio-independent OHP backscatter comparison and TMF backscatter comparisons (Sect. 3.5) suggests that the dominant altitude-dependent bias pattern identified in this study is not primarily a lidar-ratio artefact.

## 5 Conclusions

We have presented a systematic validation of the ATLID stratospheric aerosol retrieval using 895 collocated SAGE III/ISS extinction profiles and ground-based backscatter measurements from OHP and TMF, covering the period August 2024-April 2026 and spanning background, volcanic, and wildfire aerosol conditions.

The Level-1-based (K26) extinction product, derived from the ATLID scattering ratio via a with the Level-2 lidar ratio where it lies within 30-90 sr and 50 sr otherwise, shows near-zero overall bias with respect to SAGE III/ISS, with a linear regression slope of 1.04 and an overall median relative extinction difference of −2.3 % −2.2 % across all altitudes. At the integrated column level, ATLID L1 sAOD is essentially unbiased with respect to the reference, with a global mean relative sAOD bias of $-3.2\,\%$ across all matchups; the associated standard deviation of $65.7\,\%$, however, reflects a large point-to-point scatter dominated by retrieval noise under near-background aerosol loading. However, the altitude-resolved comparison comparison as a function of altitude above the local tropopause reveals a consistent vertical structure: a pronounced underestimation in the lower-to-mid stratosphere (up negative bias in the first ∼3 km above the tropopause (about −10 to $-15\,\%$), and convergence toward zero above ∼25a near-zero bias between about 5 and 15 km . This altitude-dependent bias pattern above the tropopause, and a negative bias again further up. The negative bias just above the tropopause is independently reproduced by the backscatter comparisons against OHP ($-10.6\,\%$ overall median) and TMF ($-5.5\,\%$ overall median), strongly suggesting suggesting that it is an intrinsic feature of the ATLID L1 scattering-ratio retrieval rather than an artefact of the lidar-ratio conversion.

A further noteworthy result is the better nighttime performance of ATLID L1. The daytime collocations are visibly noisierThe collocations with daytime ATLID overpasses show a larger dispersion than those with nighttime overpasses, with a relative-difference standard deviation nearly twice as large as at night (of ∼32 % versus ∼17 %, averaged over the 12-30 km range); yet the global while the median bias remains close to zero in both cases , indicating that the retrieval is still accurate in a

climatological sense. This behaviour is consistent with the HSRL capability of ATLID , which enables a much better daytime performance than a conventional elastic lidar ($-4.2\,\%$ and $-0.5\,\%$). We do not attribute this difference to either instrument: SAGE III/ISS sunrise and sunset occultations are made under the same measurement geometry, and the HSRL design of ATLID improves its daytime performance compared with elastic lidars such as CALIOP , despite the larger daytime background and associated retrieval noise (Feofilov et al., 2023)(Feofilov et al., 2023) without making it immune to daylight noise. Comparing daily zonal statistics of daytime and nighttime ATLID observations would allow a possible illumination dependence of the ATLID L1 retrieval to be quantified.

In contrast, the native ATLID Level-2 stratospheric aerosol product exhibits severe limitations across most of the dynamic range sampled in this study. Against SAGE III/ISS, the full L2 sAOD ensemble yields a regression slope of only 0.64, an artificial negative bias driven by the frequent occurrence of null retrievals (fill valueszero extinction) under low-aerosol conditions. While restricting the analysis to successful L2 retrievals artificially raises the slope to near unity, the correlation remains very weak ($R = 0.26$) because the algorithm tends to overestimate the low-sAOD background and produces spurious narrow peaks. Furthermore, the L2 product systematically overestimates peak extinction in dense volcanic and wildfire plumes. Consequently, the L1-based K26 approach introduced in Khaykin et al. (2026) provides a substantially more faithful representation of stratospheric aerosol loading across all regimes and is recommended for ATLID-based stratospheric aerosol monitoring pending future refinements of the operational L2 algorithm.

The study demonstrates that EarthCARE ATLID is capable of consistently resolving stratospheric aerosol extinction across a wide range of conditions with an accuracy of a few percent on the mean extinction profile, making it a valuable addition to the existing observing system for stratospheric aerosol. Future work should extend the validation record, incorporate additional ground-based stations at a broader range of latitudes, and undertake a dedicated lidar-ratio sensitivity study to further constrain the residual altitude-dependent bias identified here.

*Code availability.* The ATLID L1B data processing code is available at https://doi.org/10.5281/zenodo.18155346 (Kadygrov and Khaykin, 2026). The collocation and statistical analysis code used to produce the results and figures presented in this paper is available at https://doi.org/10.5281/zenodo.21282209 (Poncet, 2026).

*Data availability.* EarthCARE ATLID data are available at https://earth.esa.int/eogateway/catalog/earthcare-l1-products (last access: 5 June 2026); SAGE III data are available at https://asdc.larc.nasa.gov/project/SAGE_III-ISS/g3bssp_6 (last access: 5 June 2026); NDACC lidar data are available at https://ndacc.larc.nasa.gov (last access: 5 January 2026).

*Author contributions.* SK conceived the study, EP performed the analysis and wrote the manuscript, TL provided TMF lidar data. SK and SGB provided OHP lidar data. All authors contributed to the final manuscript.

*Competing interests.* The contact author has declared that none of the authors has any competing interests.

*Special issue statement.* This article is part of the special issue "Early results from EarthCARE (AMT/ACP/GMD inter-journal SI)". It is not associated with a conference.

*Acknowledgements.* We thank the personnel of lidar stations (OHP and TMF) for conducting lidar measurements. The French lidar stations operate under support of French Institut National des Sciences de l'Univers (INSU) of the Centre National de la Recherche Scientifique (CNRS) and of Centre National d'Études Spatiales (CNES). Part of this research was carried out at the Jet Propulsion Laboratory, California Institute of Technology, under a contract with the National Aeronautics and Space Administration (80NM0018D0004), (NASA).

*Financial support.* This research has been supported by the Agence Nationale de la Recherche (grant no. PyroStrat 21-CE01-335 0007-01), and the Centre National d'Études Spatiales (grant no. EARTHCARE).

## References


Anonymous Referee #1: Referee comment on egusphere-2026-4358, https://doi.org/10.5194/egusphere-2026-4358-RC1, 2026.

Baars, H., *et al.*: Validation of EarthCARE/ATLID aerosol profiling products with ground-based PollyNET lidars – case studies, *Atmos. Meas. Tech.*, 19, ~~3831–XXXX~~3831–3864, https://doi.org/10.5194/amt-19-3831-2026, 2026.

Cisewski, M., Zawodny, J., Gasbarre, J., Eckman, R., Topiwala, N., Rodriguez-Alvarez, O., Cheek, D., and Hall, S.: The Stratospheric Aerosol and Gas Experiment (SAGE III) on the International Space Station (ISS) Mission, *Proc. SPIE Remote Sensing*, 9241, 924107, https://doi.org/10.1117/12.2073131, 2014.

Donovan, D. P., van Zadelhoff, G.-J., and Wang, P.: The EarthCARE lidar cloud and aerosol profile processor (A-PRO): the A-AER, A-EBD, A-TC, and A-ICE products, *Atmos. Meas. Tech.*, 17, 5301–5340, https://doi.org/10.5194/amt-17-5301-2024, 2024.

Eisinger, M., Marnas, F., Wallace, K., Kubota, T., Tomiyama, N., Ohno, Y., Tanaka, T., Tomita, E., Wehr, T., and Bernaerts, D.: The EarthCARE mission: science data processing chain overview, *Atmos. Meas. Tech.*, 17, 839–862, https://doi.org/10.5194/amt-17-839-2024, 2024.

ESA Earth Online: ATLID Overview – Atmospheric Lidar, https://earth.esa.int/eogateway/instruments/atlid, last access: May 2026.

Feofilov, A. G., Chepfer, H., Noël, V., and Szczap, F.: Incorporating EarthCARE observations into a multi-lidar cloud climate record: the ATLID (Atmospheric Lidar) cloud climate product, *Atmos. Meas. Tech.*, 16, 3363–3390, https://doi.org/10.5194/amt-16-3363-2023, 2023.

Fiocco, G. and DeWolf, J. B.: Frequency spectrum of laser echoes from atmospheric constituents and determination of the aerosol content of air, *J. Atmos. Sci.*, 25, 488–496, https://doi.org/10.1175/1520-0469(1968)025<0488:FSOLEF>2.0.CO;2, 1968.

Godin-Beekmann, S., Porteneuve, J., and Garnier, A.: Systematic DIAL lidar monitoring of the stratospheric ozone vertical distribution at Observatoire de Haute-Provence (43.92° N, 5.71° E), *J. Environ. Monitor.*, 5, 57–67, ~~https://doi.org/10.1039/b211963e~~https://doi.org/10.1039/b205880d, 2003.

Haarig, M., Baars, H., König, L., Donovan, D., Ansmann, A., Khaykin, S., Ceolato, R., Cole, J., Gast, B., Floutsi, A. A., Heckmann, V. J., Hogan, R., Chantry, A., Marnas, F., van Zadelhoff, G.-J., and Wandinger, U.: The life cycle of a stratospheric smoke plume as seen from EarthCARE – tracking a plume from Canada to Europe, *Geophys. Res. Lett.*, ~~52~~53, e2025GL119977, https://doi.org/10.1029/2025GL119977, 2026.

Kar, J., Lee, K.-P., Vaughan, M. A., Tackett, J. L., Trepte, C. R., Winker, D. M., Lucker, P. L., and Getzewich, B. J.: CALIPSO level 3 stratospheric aerosol profile product: version 1.00 algorithm description and initial assessment, *Atmos. Meas. Tech.*, 12, 6173–6191, https://doi.org/10.5194/amt-12-6173-2019, 2019.

Khaykin, S. M., Godin-Beekmann, S., Keckhut, P., Hauchecorne, A., Jumelet, J., Vernier, J.-P., Bourassa, A., Degenstein, D. A., Rieger, L. A., Bingen, C., Vanhellemont, F., Robert, C., DeLand, M., and Bhartia, P. K.: Variability and evolution of the midlatitude stratospheric aerosol budget from 22 years of ground-based lidar and satellite observations, *Atmos. Chem. Phys.*, 17, 1829–1845, https://doi.org/10.5194/acp-17-1829-2017, 2017.

Khaykin, S. M., Sicard, M., Leblanc, T., et al.: Global transport of stratospheric aerosol produced by ~~the~~ Ruang eruption from EarthCARE ATLID, limb-viewing satellites and ground-based lidar observations, *Atmos. Chem. Phys.*, 26, 607–622, https://doi.org/10.5194/acp-26-607-2026, 2026.

Knepp, T. N., Thomason, L., Roell, M., Damadeo, R., Leavor, K., Leblanc, T., Chouza, F., Khaykin, S., Godin-Beekmann, S., and Flittner, D.: Evaluation of a method for converting Stratospheric Aerosol and Gas Experiment (SAGE) extinction coefficients to backscatter coefficients for intercomparison with lidar observations, *Atmos. Meas. Tech.*, 13, 4261–4276, https://doi.org/10.5194/amt-13-4261-2020, 2020.

Kovilakam, M., Thomason, L. W., and Knepp, T.: SAGE III/ISS aerosol/cloud categorization and its impact on GloSSAC, *Atmos. Meas. Tech.*, 16, ~~2709–2730~~2709–2731, https://doi.org/10.5194/amt-16-2709-2023, 2023.

Kremser, S., Thomason, L. W., von Hobe, M., et al.: Stratospheric aerosol – Observations, processes, and impact on climate, *Rev. Geophys.*, 54, 278–335, https://doi.org/10.1002/2015RG000511, 2016.

Leblanc, T., McDermid, I. S., and ~~Raspey, R. A.: Long-term measurement trends at the JPL Table Mountain Facility~~Walsh, T. D.: Ground-based water vapor raman lidar measurements up to the upper troposphere and lower stratosphere for long-term monitoring, *Atmos. Meas. Tech.*, 5, ~~2917–2931, https://doi.org/10.5194/amt-5-2917-2012~~17–36, https://doi.org/10.5194/amt-5-17-2012, 2012.

Leblanc, T., Sica, R. J., van Gijsel, J. A. E., Godin-Beekmann, S., Haefele, A., Trickl, T., Payen, G., and Gabarrot, F.: Proposed standardized definitions for vertical resolution and uncertainty in the NDACC lidar ozone and temperature algorithms – Part 1: Vertical resolution, *Atmos. Meas. Tech.*, 9, 4029–4049, https://doi.org/10.5194/amt-9-4029-2016, 2016a.

Leblanc, T., Sica, R. J., van Gijsel, J. A. E., Godin-Beekmann, S., Haefele, A., Trickl, T., Payen, G., and Liberti, G.: Proposed standardized definitions for vertical resolution and uncertainty in the NDACC lidar ozone and temperature algorithms – Part 2: Ozone DIAL uncertainty budget, *Atmos. Meas. Tech.*, 9, 4051–4078, https://doi.org/10.5194/amt-9-4051-2016, 2016b.

NDACC: Lidar Instruments – Network for the Detection of Atmospheric Composition Change, https://ndacc.larc.nasa.gov/instruments/lidar, last access: May 2026.

Shipley, S. T., Tracy, D. H., Eloranta, E. W., Trauger, J. T., Sroga, J. T., Roesler, F. L., and Weinman, J. A.: High spectral resolution lidar to measure optical scattering properties of atmospheric aerosols. 1: Theory and instrumentation, *Appl. Optics*, 22, 3716–3724, https://doi.org/10.1364/AO.22.003716, 1983.

Thomason, L. W.~~, Kovilakam, M., Schmidt, A., von Savigny, C., Deshler, T., and Rieger, L.~~ and Knepp, T.: Quantifying SAGE II (1984–2005) and SAGE III/ISS (2017–2022) ~~stratospheric aerosol measurements, *NASA Technical Reports Server*, https://ntrs.nasa.gov/citations/20230014708~~observations of smoke in the stratosphere, *Atmos. Chem. Phys.*, 23, 10361–10381, https://doi.org/10.5194/acp-23-10361-2023, 2023.

~~van Zadelhoff, G.-J., Barker, H. W., Baudrez, E., et al.: The EarthCARE mission: science data processing chain overview, *Atmos. Meas. Tech.*, 17, 839–862, https://doi.org/10.5194/amt-17-839-2024, 2024.~~

Vaughan, G., Wareing, D., and Ricketts, H.: Measurement Report: Lidar measurements of stratospheric aerosol following the 2019 Raikoke and Ulawun volcanic eruptions, *Atmos. Chem. Phys.*, 21, 5597–5604, https://doi.org/10.5194/acp-21-5597-2021, 2021.

Wehr, T., Kubota, T., Tzeremes, G., et al.: The EarthCARE mission – science and system overview, *Atmos. Meas. Tech.*, 16, ~~3581–3615~~3581–3608, https://doi.org/10.5194/amt-16-3581-2023, 2023.